Distribution Agreement

In presenting this thesis as a partial fulfillment of the requirements for a degree from Emory University, I hereby grant to Emory University and its agents the non-exclusive license to archive, make accessible, and display my thesis in whole or in part in all forms of media, now or hereafter now, including display on the World Wide Web. I understand that I may select some access restrictions as part of the online submission of this thesis. I retain all ownership rights to the copyright of the thesis. I also retain the right to use in future works (such as articles or books) all or part of this thesis.

Shruti Gupta April 11, 2017

Optimization of Dual-tropic CXCR4/CCR5 HIV-1 Entry Inhibitors and a Market Analysis

By

Shruti Gupta

Dr. Dennis Liotta
Advisor

Department of Chemistry

Dr. Dennis Liotta

Advisor

Dr. Jose Soria

Committee Member

Dr. Samiran Banerjee

Committee Member

2017

Optimization of Dual-tropic CXCR4/CCR5 HIV-1 Entry Inhibitors and a Market Analysis

By

Shruti Gupta

Dr. Dennis Liotta

Advisor

An abstract of
a thesis submitted to the Faculty of Emory College of Arts and Sciences
of Emory University in partial fulfillment
of the requirements of the degree of
Bachelor of Sciences with Honors

Department of Chemistry

2017

Abstract

Optimization of Dual-tropic CXCR4/CCR5 HIV-1 Entry Inhibitors and a Market Analysis

By Shruti Gupta

Entry inhibitors are generally prescribed after resistance to the first and second line of treatment for HIV-1 develops. Unlike other HIV-1 drugs, entry inhibitors provide a unique method of action that has a huge potential for growth in the HIV drug market. Currently, Maraviroc, which targets only one co-receptor of HIV, is the sole FDA approved chemokine entry inhibitor. Developing a novel dual-tropic entry inhibitor that would simultaneously inhibit both receptors, CCR5 and CXCR4, used by HIV-1 to enter immune cells, could effectively block the virus from entering a cell as well as inhibit evolution to a more virulent strain. Through computational modeling and structure-activity relationship analysis, modifications have been probed around the pyrazolo-piperidine scaffold to improve CXCR4-mediated viral entry inhibition, CCR5-mediated viral entry inhibition, and reduce non-nucleoside reverse transcriptase inhibition activity (NNRTI). Efforts have led to the development of compound **16**, which exhibited sub-micromolar potency against both viral tropisms and low micromolar activity against reverse transcriptase. An economic overview of the HIV drug market and the potential market for incoming entry inhibitors, especially one that is a single agent-multiple target drug, has been provided.

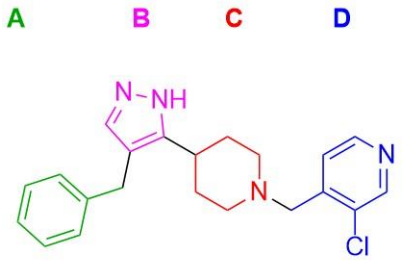

Compound 16

MAGI-HIV Infectivity Assays
HIV-1 IIIB IC_{50} = 0.2 μM
HIV-1 Ba-L IC_{50} = 0.3 μM

Mechanistic Assays
HIV-RT IC_{50} = 10 μM
CCR5 Fusion IC_{50} = 20 μM
CXCR4 Fusion IC_{50} = 9 μM

Optimization of Dual-tropic CXCR4/CCR5 HIV-1 Entry Inhibitors and a Market Analysis

By

Shruti Gupta

Dr. Dennis Liotta

Advisor

A thesis submitted to the Faculty of Emory College of Arts and Sciences
of Emory University in partial fulfillment
of the requirements of the degree of
Bachelor of Sciences with Honors

Department of Chemistry

2017

Acknowledgements

When I first stepped onto campus, I was incredibly nervous about taking Freshman Organic Chemistry, as well as about finding a community of people that not only challenged me, but also supported me and believed in me. I was lucky to have found all of that in Dr. Liotta's class, as well as in his lab. Dr. Liotta, thank you so much for giving me the opportunity to participate in SURE and continue to pursue my thesis in your lab. Thank you for all of the fatherly advice, the numerous letters of recommendation, and for being the kind, clever, and supportive mentor you are. Tony, thank you for being an incredible mentor, an avid supporter, and a brilliant scientist. Michelle, thank you for consistently pushing me to do more, being a great role model, and making sure I take care of myself. Katie, Huy, Catherine, Steve, Samesh, and the rest of the lab group – thank you for always being able to make me smile.

I want to especially thank my committee members, Dr. Jose Soria and Dr. Banerjee, for supporting me incredibly throughout my undergraduate career. You both believed in me even when sometimes I didn't believe in myself. For that, I am forever grateful. Thank you also to the rest of my incredible teachers at Emory, especially those in the chemistry department. You all helped me create a home away from home.

My parents have been my biggest support and voice of reason throughout this whole process. I dedicate my thesis to the two of you. Love you Mom and Dad. I cannot even fathom how much I have to thank the two of you for.

Table of Contents

Figures, Tables, and Schemes Table of Contents

Introduction

By the end of 2015, over 36.7 million people were suffering from human immunodeficiency virus (HIV) around the world.[1] In the United States alone, an estimated 1.2 million Americans aged 13 years and older are living with HIV infection. Approximately 13% are unaware of their infection and only 37% infected receive antiretroviral (ARV) treatment[2] (Figure 1). Most interestingly, only 30% of HIV-infected individuals have successfully suppressed the virus through treatment to less than 200 copies/mL.[3] While over two dozen FDA approved antiretroviral compounds exist to combat HIV at various points in its replication lifecycle, there is still a great need for affordable, accessible, effective options.

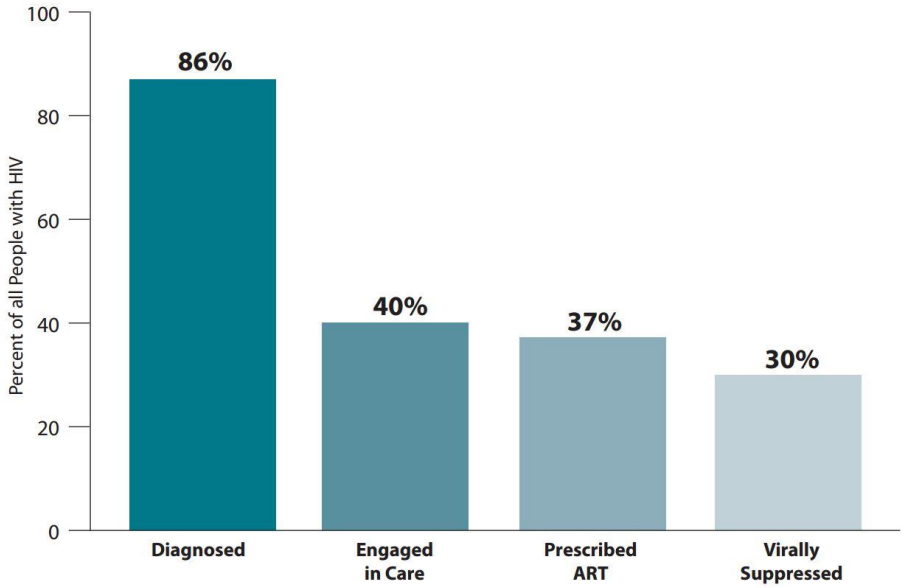

Figure 1. The population of the United States at various stages of care as of 2014.[3]

The current method of treatment aims to disrupt viral replication through combination drug therapy. Fixed-dose combination drugs hold the largest HIV drug market share and is the

most advanced method of combatting rapid drug resistance.[1] Each pill contains a cocktail of HIV-targeting compounds (generally a combination of non-nucleoside reverse transcriptase inhibitors [NNRTIs] and nucleoside reverse transcriptase inhibitors [NRTIs]) that ensures patients compliance to the drug regimen to curb resistance. Entry inhibitors, however, are not currently included in these fixed-dose pills and provide an avenue for further research.

The inhibition of viral entry is an attractive approach because it targets human chemokine protein receptors which unlike virus proteins, mutate at much slower rates. Two chemokine receptors, CCR5 and CXCR4, are used as co-receptors for HIV entry. These receptors are both seven transmembrane G-protein coupled receptors (GPCRs) that are involved in many biological functions such as chemokine signaling to mediate cellular functions like development, leukocyte trafficking, angiogenesis, and immune response. HIV infection, shown in Figure 2, begins when the virus enters the bloodstream and the viral envelope protein gp120 binds to the glycoprotein CD4 on the surface of either CD4+ T-cells or macrophages. This binding causes a conformational change on gp120 that exposes the V3 loop for binding to a secondary co-receptor for cellular entry. The virus can use either CCR5 (M-tropic, R5 virus) or CXCR4 (T-tropic, X4 virus), or both receptors (dual-tropic, X4R5 virus). Once bound to the co-receptor, the hydrophobic *N*-terminus of the transmembrane viral protein gp41 inserts into the target cell membrane and delivers the viral payload.[4,5,6,7]

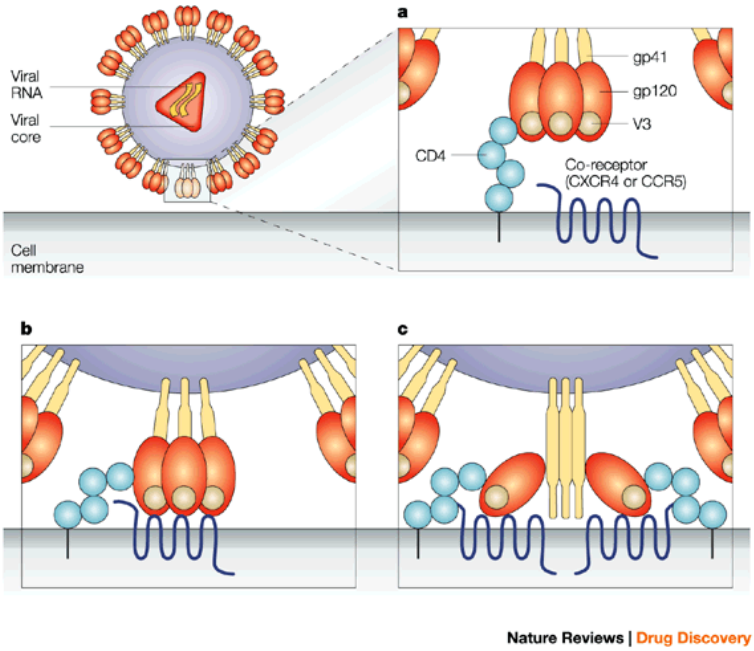

Figure 2. HIV entry into an immune cell.[8]

Only two FDA approved entry inhibitors exist on the market: Maraviroc (Selzentry®), a spirodiketopiperazine CCR5 antagonist[5], and enfurvitide (Fuzeon®), which binds to gp41 of HIV to prevent fusion with the target cell membrane (Figure 3). Enfurvitide is prescribed in cases where patients are experiencing HIV-1 replication despite ongoing anti-retroviral (ARV) treatment.[9] Because gp41 is a viral target, resistance to enfurvitide emerges rapidly.[5] On the other hand, maraviroc, which has low nanomolar concentration CCR5 antagonism activity, is used for ARV naïve patients who have undergone an expensive tropism exam to ensure they carry the M-tropic strain. In earlier studies, patients with T-tropism or dual/mixed tropism that took maraviroc saw disease progression accelerate. In fact, patients harboring only the M-tropic strain found that use of maraviroc for an extended period resulted in selection of the more virulent dual-tropic and T-tropic strains of the virus in 57% of patients within 5 years.[5,10]

To date, no FDA approved entry inhibitors that target the co-receptor CXCR4 exist.[11] Two CXCR4 antagonists AMD3100 and AMD11070 have entered clinical trials as T-tropic HIV-1 entry inhibitors, however both studies were ultimately terminated due to adverse effects (Figure 3). AMD3100 exhibited dangerous levels of liver and cardiotoxicity for chronic treatment, although it was approved for stem cell mobilization.[12] AMD11070 showed off-target effects, however in the last clinical trial it was found that three of the four patients responded to therapy by showing a tropism shift from dual/mixed tropic viruses to exclusively R5 virus by day 10.[13]

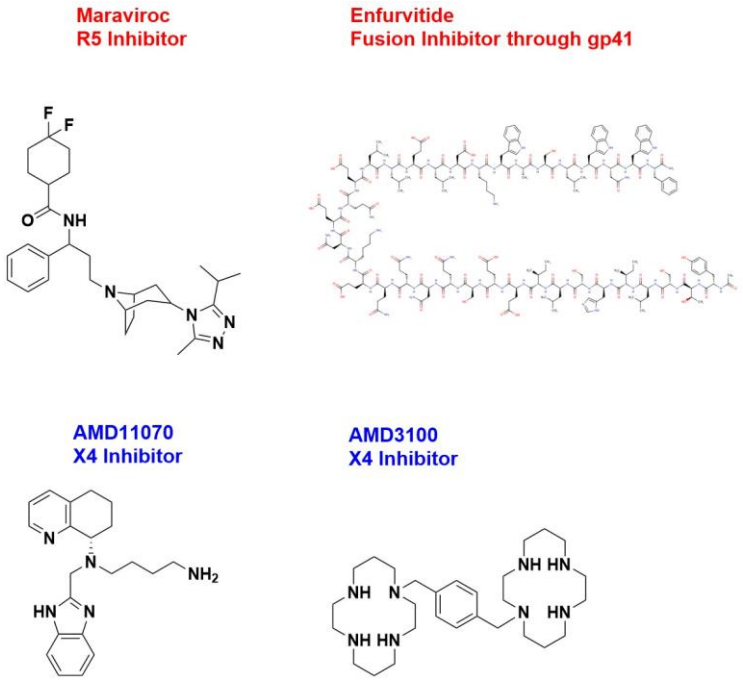

Figure 3. Current Entry Inhibitor Chemical Structures.[11]

In 2005, about 12-19% of treatment-naïve individuals exhibited dual/mixed strains and less than 1% exhibited the X4 strain. Of treatment-experienced individuals, dual/mixed and X4

prevalence jump to 22-48% and 2-4%, respectively.[10] Since then, resistant strains has only surged. The tropism shift from M-tropic to T-tropic and the existence of dual/mixed tropic strains of HIV-1, suggests the innate importance of building an entry inhibitor that can simultaneously target both CCR5 and CXCR4 with a low toxicity profile (Figure 4).

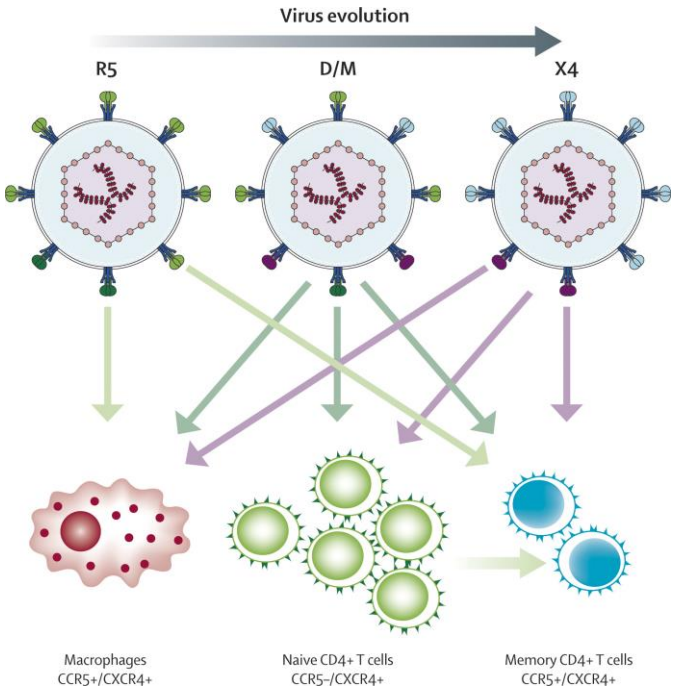

Figure 4. Cellular tropism and viral evolution. D stands for the dual-tropic R5X4 viral strain, and M stands for mixed tropism of both R5 and X4 viral strains within one patient.[10]

Therefore, we have made efforts towards the discovery and synthesis of a singular compound that targets both co-receptors. This type of dual-tropic compound could also be cost effective and create a new niche in the HIV drug market where entry inhibitors could transition from a tertiary method of ARV treatment to a primary one, which I will explore further in the next section of this report.

HIV Drug Market Economic Analysis

The $9.3 billion (2012) [14] United States HIV therapeutics market is largely dominated by a handful of treatments and companies. The oligopoly economic model explains the increasingly high costs for HIV treatment. Gilead Sciences itself held 45.1% of the market share in 2013 as the sole producer of the single tablet regimen, fixed dose combination drugs (STR FDC) currently in the market, which includes Atripla, Complera, and Stribild. Patent protection for seven of the eight leading antiretroviral (ARV) drugs will expire by 2018, which will expedite the growth for the generic HIV drug market while the market overall will steeply decline due to pricing pressures (expected at $6.8 billion in 2018).[15] In order for the market to maintain sufficient incentives for HIV drug research, the needs of the current population have to be addressed. These immediate needs include affordable and easily accessible drugs, drugs with novel mechanisms of action and reduced toxicity, and drugs that alleviate the burden of the daily treatment regimen and prevent evolution of drug-resistant HIV strains.[14] We believe a dual-tropic candidate would fit all three of these classifications.

Public Policies

According to the latest WHO HIV treatment guidelines from 2016, ARV therapy is recommended for any adult living with HIV at any CD4 cell count with priority shown to patients with severe HIV clinical disease (cell count <350 cells per/mL).[16] This is vastly different from the 2013 guidelines suggesting ARV should be initiated at a CD4 cell count of 500 cells per/mL, with focus on those with less than 350 cells per/mL.[17] Globally, this expands the ARV-

eligible population from 28 million to 37 million patients. Focus is also shifted to preventative drugs, such as Truvada.[18]

The 2017 USA domestic budget set aside $27.5 billion for HIV-related items within the US, such as care and treatment, cash and housing services, prevention, and research (Table 1). Medicare, Medicaid, and the Ryan White HIV/AIDS Program are, in that order, the largest federal funders of HIV care and treatment. With costs and the demand for care rising, funding continues to increase every year. $900.3 million of that money was set aside specifically for Ryan White's AIDS Drug Assistance Program (ADAP), which provides access to subsidized medications for poor and uninsured HIV-infected patients.[19]

Table 1. Federal Funding for HIV/AIDS by Category, FY 2011 – FY 2017 Request (US$ Billions).[19]

Category	*FY 2011*	*FY 2012*	*FY 2013*[a]	*FY 2014*	*FY 2015*	*FY 2016*	*FY 2017 Request*
Domestic	**$21.8**	**$22.0**	**$22.5**	**$23.9**	**$25.5**	**$26.4**	**$27.5**
Care	$15.3	$15.5	$16.1	$17.4	$18.9	$19.7	$20.8
Cash/Housing	$2.7	$2.8	$2.9	$3.0	$3.0	$3.0	$3.1
Prevention	$0.9	$1.0	$0.9	$0.9	$0.9	$0.9	$0.9
Research	$2.8	$2.8	$2.7	$2.7	$2.7	$2.7	$2.7
Global	**$6.5**	**$6.4**	**$6.3**	**$6.6**	**$6.6**	**$6.6**	**$6.6**
TOTAL	**$28.3**	**$28.5**	**$28.8**	**$30.5**	**$32.1**	**$33.0**	**$34.0**

NOTES: (a) indicates FY 2013 includes the effects of sequestration.

$2.7 billion is designated for research.[19] US donors in the public, private, and philanthropic sectors contribute to more than 90% of the funds spent on HIV research. Most notable are the NIH, Gilead Sciences, and the Bill and Melinda Gates Foundation. Over 50% of research investment is used for therapeutics, as opposed to vaccines, prophylaxis, etc.[15] The USA's focus on research further exemplifies the country's focus on healthcare quality,

sometimes in place of equity. It is a challenge to balance the intellectual property profitability required by big pharmaceutical companies to continue their research as well as to allow for generic companies to increase accessibility to those drugs immediately for the greater good.

Market Demand

Although North Americans comprise only 4% of the worldwide share of people living with HIV, they hold a 41% share of the global HIV therapeutics market.[15] Even then, as shown in Figure 1, only 30% of HIV-infected patients are considered virally suppressed.[3] About 48,000 new cases of HIV are diagnosed every year in North America, however new cases of HIV-positive children have declined to below 200 in 2012. ARV drugs for pregnant women and early infant prophylaxis have contributed to this progress.[15]

With the new WHO guidelines, the number of eligible ARV patients has greatly increased. Coupled with the technological advances and accessibility of the HIV diagnostics market, the high costs of HIV drugs and the increase in life expectancy for HIV-positive patients have contributed to the continuous growth in the overall market size throughout the years. The lack of competition, however, suggests that supply is more limiting than the demand for HIV treatment. Although demand for HIV therapeutics continues to rise in the United States, the market is expected to experience a compound annual growth rate (CAGR) of -2.1%, representing a $7.6 billion market in 2013 dropping to $6.8 billion in 2018. From 2017 onwards, the decline will largely be due to the patent expiration of Janssen's Prezista (darunavir) and Bristol-Myers Squibb's Reyataz (atazanavir). Due to the patenting of new formulations of STR

FDC drugs which can combine these drugs in novel, synergistic methods, demand would have to shift to new treatments for companies to continue to profit.[15]

The market has been seeing a major decline in the shares of the top eight leading drugs in 2012 (Table 2). First, the original eight leads are being replaced by newer, more potent, and less toxic drugs like Stribild, Complera, and Trivicay. Second, the generic drug market has been expanding, as shown in the Others category, as many of the former leads lose their patents. Although newer drugs and formulations are becoming more clinically popular, the presence of generic, cheaper options may alter insurance policies. STR FDC drugs are also more cost effective than paying for individual component drugs. Therefore, although the accessibility of treatment may increase in terms of cost and newer drugs will offset some lost revenue from the shift to generics, there is still projected to be a decline in the overall market by 2018.

Table 2. Market shares suggest demand transition to newer drugs and generics. [15]

HIV MARKET SHARE BY LEADING DRUGS (%)

Drug	2012	2013	2018
Atripla	20.4	19.4	7.6
Truvada	18.9	17.1	9.2
Reyataz	8.7	8.3	3.3
Isentress	8.6	8.5	8.2
Prezista	8.4	8.4	6.8
Epzicom	6.0	6.1	2.9
Kaletra	5.8	5.3	1.6
Viread	4.8	5.2	3.9
Intelence	2.1	2.1	2.8
Complera	1.9	3.8	8.8
Stribild	0.3	2.7	17.8
Tivicay	0.0	0.4	6.7
Others	14.1	12.7	20.4
Total	100.0	100.0	100.0

Treatment-experienced patients (37% of the population), unlike treatment-naïve patients, are often out of options for their resistant viruses and are in need of innovative therapies. New WHO guidelines are attempting to incentivize research for this population subset.[15] For treatment-naïve patients, the WHO recommends the first line of treatment to include two NRTI's and one NNRTI. The second line replaces the NNRTI with a more robust protease inhibitor. The third line of defense then becomes other classes of drugs, including entry inhibitors.[20] As of 2013, however, only about 72% of patients adhere to their regimen after five years.[15] Due to the quickly evolving virus, there is a greater demand for drugs that can either prolong evolution or ease the burden of following the regimen. A dual-tropic entry inhibitor, unlike maraviroc, could potentially be used for treatment-experienced patients, as part of the first line of defense, or even as a prophylactic.

Market Supply

By the end of 2015, only 37% of all patients suffering from HIV in the United States were receiving ARV therapy.[1] Affordability is a major contributor to the lack of access to drug therapy. Five companies are expected to dominate over 95% of the HIV therapeutics market by 2018, as shown in Figure 5.[15] Taking the declining market into account ($7.6 to $6.8 billion in 2018), Gilead remains relatively flat while Viiv is expected to grow. Both Bristol Myers-Squibb and AbbVie are projected to hit a steep decline, while Merck and Janssen experience a slight decline. The 'Others' category represents a slight increase in competition immediately after patent expiry.

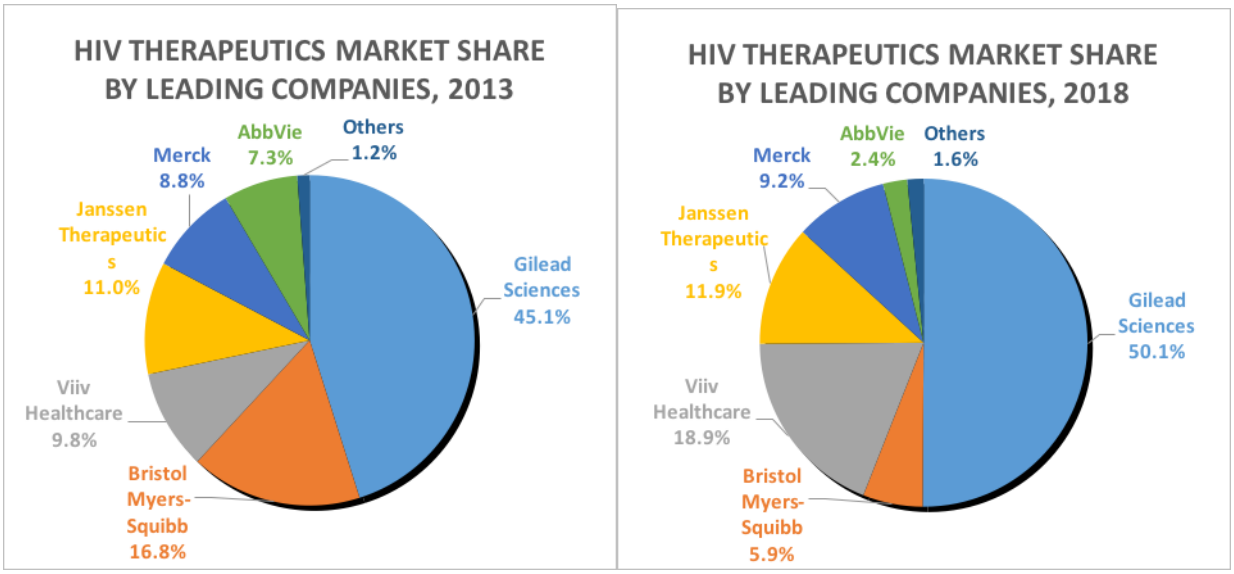

Figure 5. HIV therapeutics display a small projected rise in the 'Others' category, suggesting some enhanced competition immediately after patent expiry.

As patents begin to expire (Table 3), pharmaceutical companies have an incentive to evergreen by filing subsequent patents with 'novel features' through STR FDC drug creation. In that way, they can protect their profit via newer technologies stemming from existing compounds.

Table 3. Seven of eight top leading drugs will become available for generic entry by 2018. [15]

LEADING ARV DRUGS ON PATENT CLIFF

Drug	Year of Patent Expiry
Atripla	2018*
Truvada	2017*
Viread	2017
Prezista	2015
Reyataz	2017
Kaletra	2016
Sustiva	2015

When given the chance, generic drugs will gain popularity as they are slowly approved through the abbreviated new drug application (ANDA) by the FDA. The United States has one of the most rapid, estimated declines in original brand sales at the time of generic entry, down to 70% of the total after 1 year for a sample of pharmaceuticals in the past, especially due to the Waxman-Hatch Act.[21] When generic drugs enter, the market will shift slightly from an oligopoly to one with added competition. Supply and accessibility will then increase as market prices are most likely to decline.[21] Due to the shift to newer drugs like Complera (Table 2) and patent evergreening, however, insurance policies and WHO recommendations can have unpredictable impacts on market prices consumers may experience. For example, copays may make buying multiple generic drugs as opposed to one STR FDC less desirable for a patient.[15]

Although the demand for entry inhibitors is the lowest of all the classes of HIV drugs, as shown in Table 4, it is expected to have the greatest growth due to novel methods of action being researched.[15] It is also a pertinent option for treatment-experienced patients. Currently, there are three major entry inhibitors in clinical trials that may enter the market by 2018. These include ibalizumab (Phase III), fostemsavir (Phase III), and cenecriviroc (Phase IIB).[11] Cenecriviroc is a potential dual-tropic inhibitor, however it focuses on CCR5 and CCR2 (potentially related to inflammatory pathways and Alzheimer's). Fostemsavir and ibalizumab affect gp120 and CD4, respectively, however gp120 is a quickly evolving viral protein and CD4 is used in a variety of normal cellular functions.[4,5,11] The other entry inhibition competitor, maraviroc, is expected to experience a decline in profits to $240 million by 2018. The costly tropism test tends to limit its first line use and profitability, and its revenue is projected to

continue to decline beyond 2018. In the United States, the costs of second or third line of defense treatments are about twice the cost of the first line of defense.[15] Maraviroc originally had at least a ten step synthesis, and in 2015, a four step synthesis utilizing C-H functionalization was established with expensive reagents.[22] These competitors suggest the need for an entry inhibitor that negates the need for a tropism test, prolongs evolution, limits toxicity, and can be relatively affordable.

Table 4. Entry inhibitors are projected to almost double their market value from 2012 by 2018. [15]

HIV THERAPEUTICS MARKET BY DRUG CATEGORY, THROUGH 2018 ($ BILLIONS)

Drug Category	2012	2013	2018	CAGR% 2013-2018
Nucleoside/nucleotide reverse transcriptase inhibitors (NRTIs)	5.8	5.8	3.9	-7.8
Protease inhibitors (PIs)	4.9	4.8	2.6	-11.4
Single tablet regimen fixed-dose combination (STR FDC)	4.0	4.7	7.8	10.6
HIV integrase strand transfer inhibitors (INTIs)	1.5	1.6	3.5	16.2
Non-nucleoside reverse transcriptase inhibitors (NNRTIs)	1.0	1.1	1.3	3.0
Entry inhibitors	0.3	0.2	0.7	28.3
Total market	17.5	18.2	19.6	1.5

Summary

As federal funding continues to increase for HIV/AIDS care in the USA each year (Table 1), the demand for novel therapeutics continues to increase due to better diagnostic capabilities, longer lifespan, and the new WHO and NIH guidelines.[23] There is a growing need for affordable, accessible pharmacological targets that can prolong evolution and provide a novel method of treatment for already resistant viral strains in treatment-experienced patients.

The oligopolistic market (Figure 5) is looking for innovative treatments as seven of the leading eight ARV drugs lose their patents by 2018 (Table 3).[14] As newer drugs and generics start to increase competition (Table 2), entry inhibitors provide an avenue of untapped growth (Table 4). Research efforts that overcome the current barriers to utilizing entry inhibition, like tropism tests and ease of synthesis, could prove fruitful.

Results

Molecular Modeling

The first step in our research was to discover a scaffold with dual-tropic activity. A Bayesian statistical model was constructed for CXCR4 and CCR5 and were used to virtually screen the Aldrich Market Select library (2012, Q3; ~5.6 million compounds). The compounds were scored then ranked using the distance-from-optimal method. The top 300 compounds were inspected, and 14 of the most drug-like/synthetically accessible molecules were purchased. The molecules were screened in an anti-HIV activity assay to determine their potency against both CXCR4 and CCR5 expressing strains. The screening identified a moderately potent CXCR4/CCR5 dual entry inhibitor, compound **1**, which contained a pyrazole-piperidine moiety. A second round of screening of compounds was conducted around the pyrazole-piperidine substructure. 24 structurally similar compounds were purchased and tested, and from them eleven compounds exhibited dual-tropic activity. Of the eleven, compound **1** containing a 4-pyridine ring became our lead structure (Figure 6). Compound **1** was examined in MAGI HIV-1_{IIIB} (X4 tropic virus) and HIV-1_{Ba-L} (R5 tropic virus) assays, HIV-RT assays, and CXCR4 and CCR5 fusion assays and was found to mildly inhibit reverse transcriptase in addition to inhibiting CXCR4 and CCR5.[24]

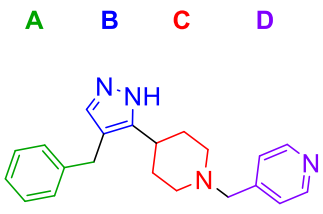

Compound 1

MAGI-HIV Infectivity Assays
HIV-1 IIIB IC_{50} = .8 μM
HIV-1 Ba-L IC_{50} = 3.8 μM

Mechanistic Assays
HIV-RT IC_{50} = 9 μM
CCR5 Fusion IC_{50}=35 μM
CXCR4 Fusion IC_{50} = 52 μM

Figure 6. Anti-HIV profile of Compound **1**.[24]

Our efforts since have been focused on increasing anti-viral potency and determining the mechanisms of action of the scaffold's structural elements that allow us to hit three anti-viral targets. Compound **1** was bound to models of CXCR4, CCR5, and HIV-1 reverse transcriptase, as shown in Figure 7, using the methods described in Cox (2015).[24] This modelling allowed us to further ascertain future targets of interest and correlate our predictions with biological assay results.

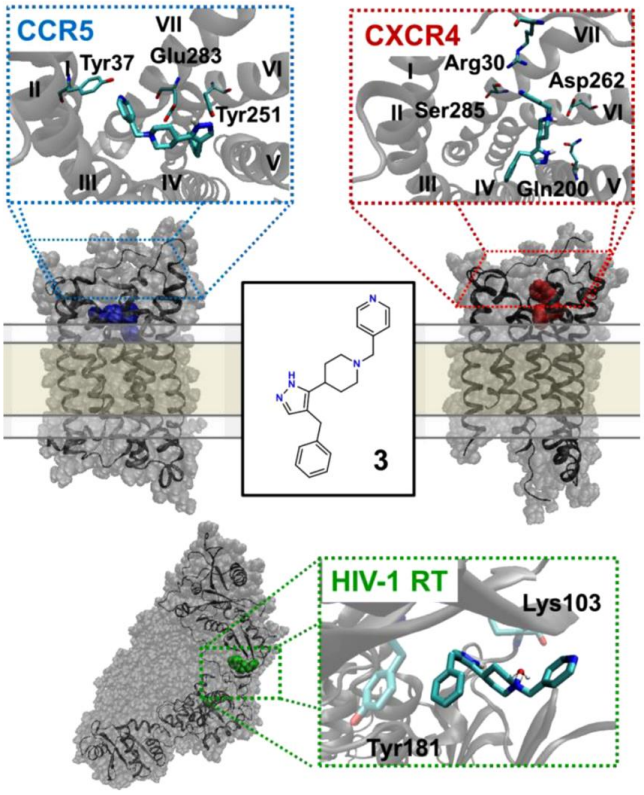

Figure 7. Our compound **1** is equivalent to this compound *3*. Adapted from Cox (2015). "Predicted binding mode of compound *3* to the three biological targets. In all models, the piperidine nitrogen is cationic and the tautomeric state of the pyrazole positions the hydrogen nearest the piperidine ring. The model of compound *3* complexed to the extracellular binding pocket of CCR5, derived from the CCR5:Maraviroc cocrystal structure as a template, spans the entire orthosteric site (blue). The model of compound *3* binding to the extracellular binding pocket of CXCR4 using the CXCR4:CVX15 crystal structure displays interactions only in the major subpocket (helices I, V, VI, and VII) (red). Predicted U-shaped binding mode of compound *3* binding to HIV-RT p66 subunit demonstrates interactions with Tyr181 and water-mediated interactions with Lys103 (green)."[24]

From first glance, compound **1** can be disconnected into four distinct moieties (Figure 6). The necessity of the A and C rings were determined from previous work. Using molecular computational analysis of published CXCR4 and CCR5 crystal structures shown in Figure 7 along with the SAR shown in Scheme 1, the D-ring was found to be pertinent to chemokine-blocking

activity. Deletion resulted in a ten-fold loss in potency between **1** and **3**. The favorable bonding interaction with Tyr37 in CCR5 and Ser285 in CXCR4 can be optimized through D-ring alterations. In the process of computational analysis, we also predicted the B-ring's potential for stronger hydrogen bonding interactions with Tyr251 in CCR5 and Gln200 in CXCR4. This was especially proven due to the loss of activity in CXCR4 in vitro when comparing **1** and **2** (Scheme 1). As a result, we are synthesizing analogs of the B and D-ring in hopes of increasing potency while maintaining low levels of toxicity.

Scheme 1. SAR depicting the relevance of the B- and D-rings. Compounds developed by Anthony Prosser.

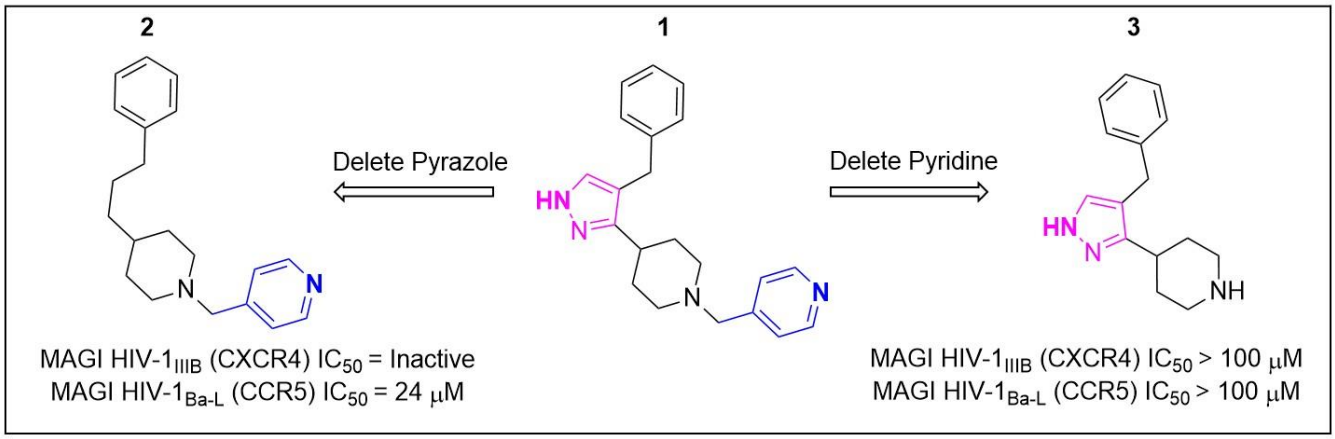

Synthesis of D-ring Derivatives

The synthesis of **1** began with the conversion of commercially available ethyl 1-benzylpiperidine-4-carboxylate **4** into the Weinreb amide (Scheme 2). The Weinreb amide was treated with excess phenethylmagnesium bromide to afford compound **5**. The addition of sodium hydride, 15-crown-5, and methyl formate to the ketone formed a 1,3-dicarbonyl

intermediate. The addition of hydrazine in the presence of methanol installed the pyrazole ring, where $\mathbf{R_1}$ for this series is equal to NH. Hydrogenation reaction of **6** removed the benzyl protecting group cleanly and the resulting product was used without purification. The final reaction was a reductive amination with 4-pyridine-carboxyaldehyde to form final product **7**.

Scheme 2. General Synthesis of Scaffold, showing compounds **4**, **5**, **6**, and **7**.

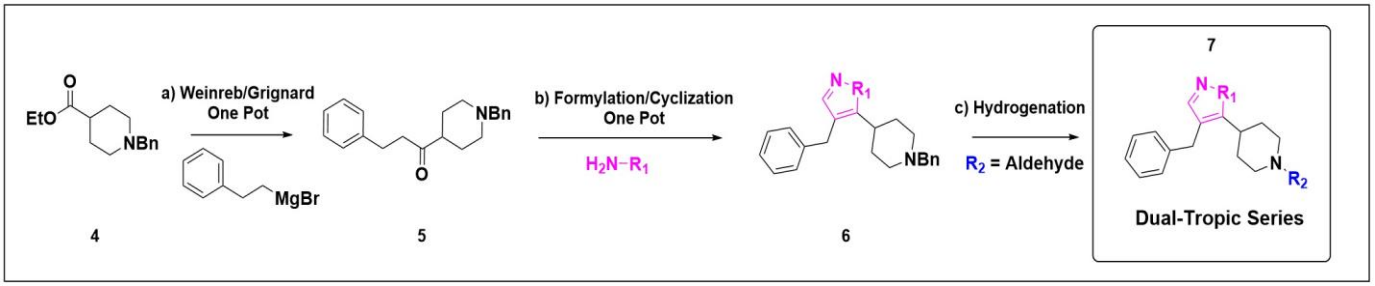

Reagents: (a) *N*,*O*-dimethylhydroxylamine hydrochloride, phenethylmagnesium bromide, THF; (b) NaH, 15-crown-5, methyl formate, MeOH, H_2NOH-HCl or N_2H_4, THF; (c) 10% Pd/C, *t*-BuOH; $NaBH(OAc)_3$, R_2-CHO, DCM. Developed by Anthony Prosser.

Lead compound **1** was initially modeled in both receptors CXCR4 and CCR5 to understand the relationship between potency and structure. The modeling studies bound in CXCR4 was difficult and provided poor correlations between ligand structure and activity, and thus a CCR5-derived model was explored by other members in the group. Compound **1** was modeled in the maraviroc-binding pocket of the CCR5 receptor and the top-scoring pose showed that **1** extended across most of the binding pocket at alpha-helixes I, II, III and VII. As such, **1** formed several important interactions, as shown in Figure 8A. The D-ring 4-position on the pyridine formed hydrogen bonding interactions with Tyr37, the C-ring piperidine interacted with Glh283, and the molecule also interacted with Tyr251 (not shown). Based on the modeling data, an initial structure-activity relationship (SAR) study around the D-ring was investigated.

Several D-ring derivatives were synthesized and each compound was assessed in the MAGI HIV-$1_{Ba\text{-}L}$ (R5-tropic) and MAGI HIV-1_{IIIB} (X4-tropic) assays to ascertain overall anti-viral activity (data not shown). The derivatives were then docked into the same binding pocket of **1** to assess if there was good correlation between the activity and the modeling pose. Combining the results from the first round of SAR data with the ligand docking study, we predicted a second generation of D-ring analogs that could form better interactions within the allosteric pockets of CCR5 (**8** shown in Figure 8B).

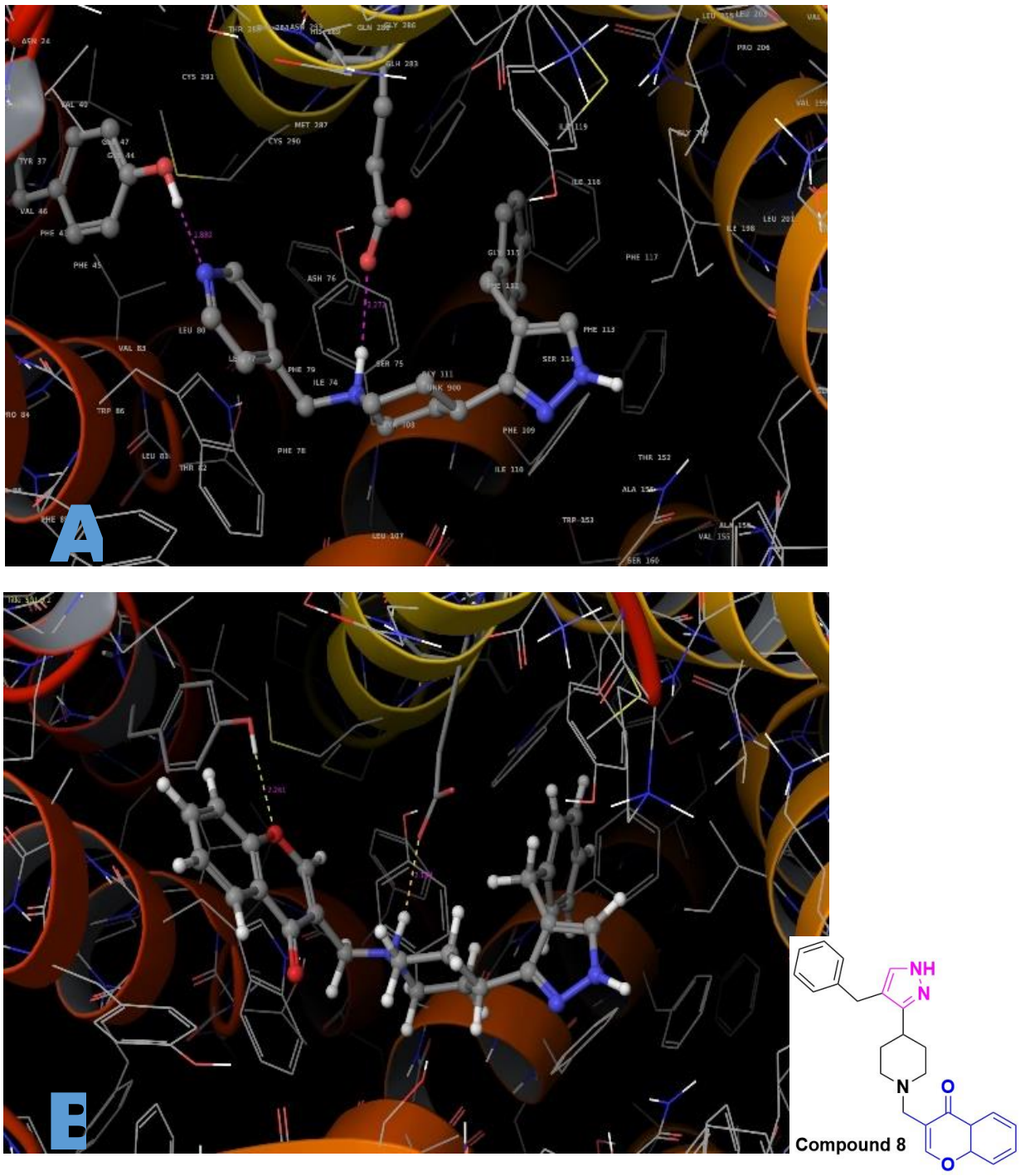

Figure 8. Glide docking of dual-tropic inhibitors in the active site of CCR5 receptor, 4MBS PDB. (A) Compound **1** shows hydrogen bonding with Tyr37 and Glh283 (B) Compound **8** showed the same interactions with varying distance. Inhibition at 10 µM was 37% for HIV-1_{Ba-L} and 17.2% for HIV-1_{IIIB} in the MAGI assay, which was less potent than Compound **1**.

In the second round of SAR, compounds **9**-**16** were synthesized using the general route presented in Scheme 2 (Table 5). Each compound was assessed in the MAGI HIV-$1_{Ba\text{-}L}$ (R5-tropic) and MAGI HIV-1_{IIIB} (X4-tropic) assays to ascertain overall anti-viral activity. Toxicity was determined via cell count of non-infected MAGI cells. In addition, NNRTI μM IC_{50} assays were performed to further assert method of action for the most potent compounds (Table 5). Based on our model the MM-GBSA (kcal/mol) energy was calculated for our compounds and seemed to predict in the $HIV_{Ba\text{-}L}$ strain with good correlation ($r^2 = 0.77$).

Table 5. Profiling of D-ring derivatives.

#[a]	R=	Prime MM-GBSA ΔG Bind (kcal/mol)	MAGI Assay IC_{50} μM		RT IC_{50} μM	TC_{50} μM
			Ba-L	IIIB		
1	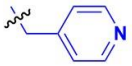	87.33	3.8	0.8	9	>100
9	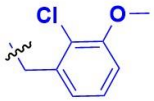	97.95	1.3	2.0	1.5	24
10	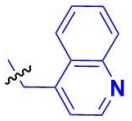	94.69	0.84	1.4	2.8	>30
11	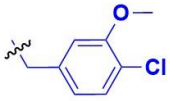	90.82	94%[b]	85%[b]	77%[b]	87%[b]
12		87.75	58%[b]	41%[b]	-	95%[b]
13	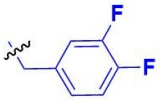	85.15	5.4	18	-	32
14		84.76	6.6	16	-	49
15	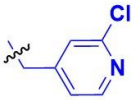	96.76	0.28	0.17	9.6	34
16	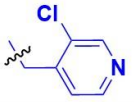	95.79	0.21	0.14	10.	67

[a] Synthesized with purity >95%

[b] Due to more potent derivatives, only preliminary MAGI assay inhibition at 10μM was determined

[c] Synthesized by Anthony Prosser

Compounds **10** and **12** were synthesized to probe the chemical space around the D-ring. Isoquinoline **10** had good potency in both strains of HIV while pyrazolopiperidine **12** had a slight loss in activity which indicated that the *p*-nitrogen moiety may be a key interaction for activity. To further explore this the *p*-methylbenzene derivative **14** and difluoro **13** were synthesized and a loss in potency in both compounds reaffirmed our hypothesis. Compounds **9** and **11** investigated the position of a chlorine around the ring. The potency improved for the Ba-L strain when the chloro was in the ortho-position, but was less potent in the IIIB strain. The chloro in the *para*-position in **11** was at best active by 94% at 10 µM. Compounds **15** and **16** were synthesized to probe both characteristics simultaneously, the *p*-nitrogen and the chloro group, to improve potency in the MAGI assay. The potency for compounds **15** and **16** in the MAGI assays were gratifyingly lower than the initial lead compound **1** in both strains of HIV.

Table 6 shows several potent dual-tropic compounds that have been synthesized. Their method of action was further investigated using a fusion assay as these compounds seemed to hit CXCR4, CCR5, and reverse transcriptase (RT). Compounds **9** and **10** were potent against RT at sub-micromolar concentration, but both compounds were inactive in the fusion assay against both strains of HIV leading to the possibility that most of the activity could be a result of RT. Between compounds **1**, **15**, and **16**, compound **16** was the most active in the fusion assay with low RT activity. Therefore, **16** was chosen as the optimal D-ring substituent, especially as the *meta*-chloro on **15** presented a metabolic liability.

Table 6. Profiling of lead D-ring compounds.

Table 6. Profiling of Two Sub-Series

#	R=	MAGI Assay IC_{50} μM		RT IC_{50} μM	Fusion Assay IC_{50} μM		Method of Action
		Ba-L	IIIB		CCR5	CXCR4	
9[a]	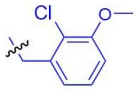	1	2	2	>40	>40	NNRTI
10[a]	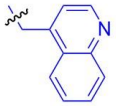	0.8	1	3	>40	>40	
1[b]	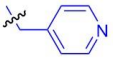	4	0.8	9	35	52	CXCR4 CCR5 NNRTI
15[b]	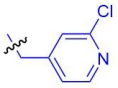	0.3	0.2	10	19	14	
16[b]	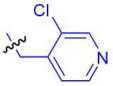	0.2	0.1	10	20	9	

[a] Synthesized by SG
[b] Synthesized by ARP

Synthesis of Novel B-ring

While our molecule interestingly exhibited three anti-viral methods of action, the optimization of all three targets CCR5, CXCR4, and viral reverse transcriptase is difficult and undesirable. Moreover, **1** failed to inhibit the K103N/Y181C mutant of reverse transcriptase, and is therefore clinically less relevant.[24] In addition, lead compound **16** inhibited reverse transcriptase less potently than the other two targets. For these reasons, efforts towards removing reverse transcriptase activity was attempted. Molecular modeling of compound **16** within the aminopyrimidine NNRTI binding pocket of the crystal structure of HIV-RT was investigated (Figure 9A; PDB: 3M8Q). The 4-position on the D-ring formed interactions with

Val106, the A-ring exhibited pi-stacking interactions with Tyr181, and the B-ring pyrazole ring nitrogens interacted with Lys101. The RT crystal structure was chosen for the aminopyrimidine's structural similarity to **16**, which can be seen in the overlay in Figure 9B.

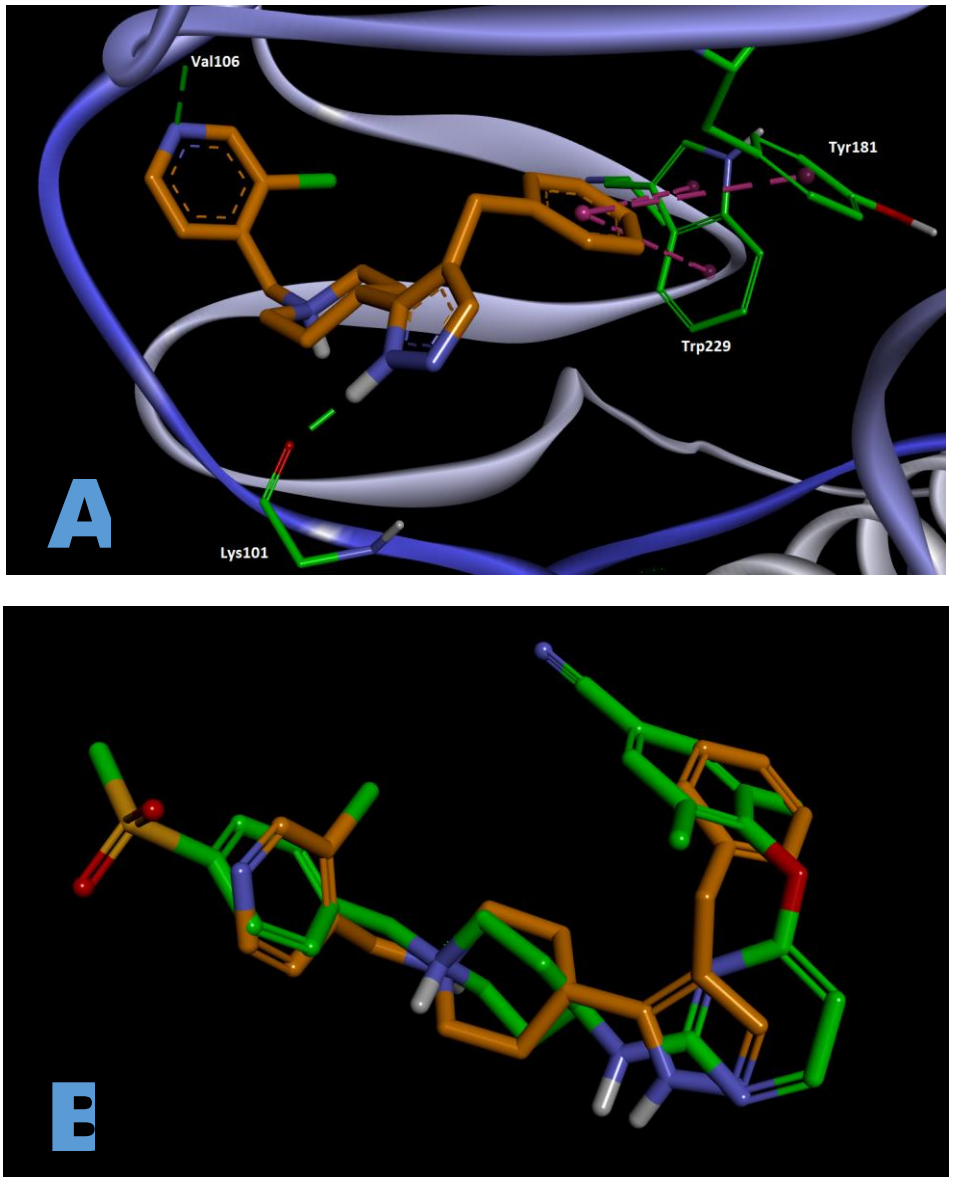

Figure 9. Glide docking of dual-tropic inhibitor **16** in the active site of RT receptor, 3M8Q PDB. (A) Compound **16** shows hydrogen bonding with Val106 and Lys101 (B) Compound **16** is overlayed with aminopyrimidine, the natural crystal structure ligand, to show structural similarity.

The Lys101 interaction allowed us to hypothesize that replacing the nitrogen with an oxygen through an isoxazole moiety would reduce reverse transcriptase activity by interrupting the Lys101-pyrazole interaction. Docking studies of **16** into the CCR5-receptor model ensured that modifications to the B-ring would not interfere with any significant interactions, and thus synthetic efforts were made to replace the pyrazole with an isoxazole (Scheme 3).

Scheme 3. Synthesis of B-ring analog.

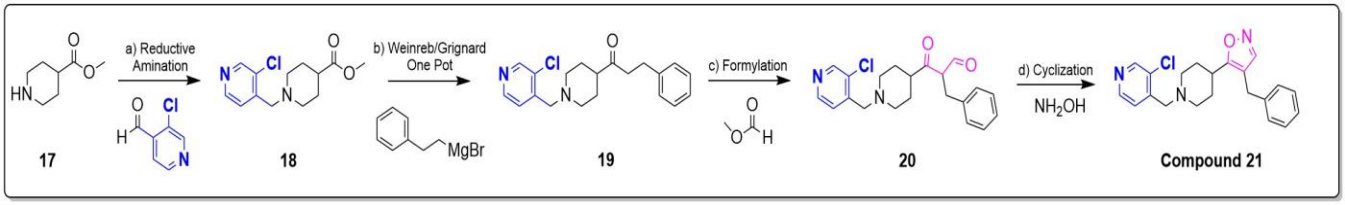

Reagents: (a) $NaBH(OAc)_3$, aldehyde, DCM; (b) *N*,*O*-dimethylhydroxylamine hydrochloride, phenethylmagnesium bromide, THF; (c) NaH, 15-crown-5, methyl formate, MeOH, THF; (d) $H_2NOH•HCl$, THF, and driven to completion with acetic acid at 65°C .

The A, C, and D-ring moieties that gave the best activity were used in the synthesis of the isoxazole B-ring. The synthesis began with the reductive amination between piperidine **17** and the 3-chloro-4-pyridinecarboxaldehyde (Scheme 3). The ester of **18** was treated with the Weinreb salt followed by treatment with phenethylmagnesium bromide at 0°C to furnish ketone **19**. The addition of sodium hydride, 15-crown-5, and reagent grade methyl formate to ketone **19** in THF then formed a 1,3-dicarbonyl intermediate **20**. The crude product was then cyclized using NH_2OH-HCl, but only the oxime was isolated. Cyclization of the oxime was driven to completion with acetic acid at 65°C to afford the final product **21**. This molecule, as well as other B-ring analogs, will be further synthesized by members of our group and tested for reduction of reverse transcriptase activity.

Conclusions

An effort to create a singular compound that can simultaneously inhibit CCR5 and CXCR4 to block HIV from entering a cell has been undertaken. This type of entry inhibitor would provide the HIV drug market with a novel method of action as a differentiated product. Beginning from a virtual screening using Bayesian models, a pyrazolo-piperidine scaffold was identified and over ten modifications to the B- and D-ring were explored to create a series of dual-tropic compounds. The lead compound **16** was developed with sub-micromolar MAGI antiretroviral activity for both the R5 and the X4 strains of HIV-1 with weak RT activity (Figure 10). Various analogs of the compound, including an isoxazole B-ring moiety, were synthesized to dial out RT activity. The ease of synthesis for this series (~3 steps) makes for a quick and affordable route while its ability to target dual-tropisms would contribute to the fight against the evolution of HIV. In future work, our group will continue to modify the scaffold in search for a dual-tropic compound with nanomolar potency, low toxicity profile, and diminished reverse transcriptase activity.

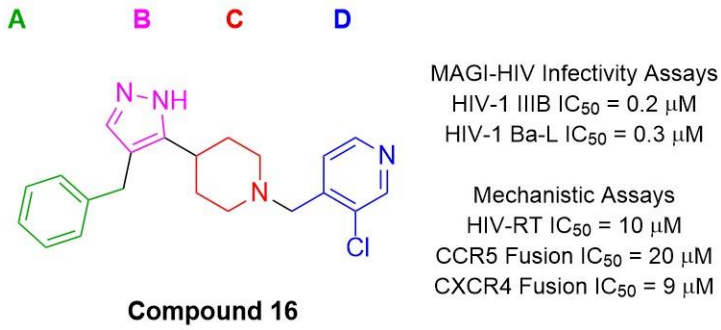

Figure 10. Profile of lead compound **16.**

Experimentals

General Hydrogenation Procedure. To a solution of the substrate in *t*-BuOH (0.1 M) and AcOH (0.01 M) is added Pd/C (10-50% by mass). The reaction was hydrogenated under an atmosphere of H_2 between 45-55 psi on a Parr hydrogenator overnight. Upon completion the H_2 was purged in vacuo and then flushed with argon. The crude reaction mixture was then filtered through two fluted pieces of filter paper and concentrated in vacuo. The mixture was then diluted with brine and DCM followed by basification with 10% NaOH. The layers were separated and the aqueous layer extracted with DCM (3 times). The organic layers were combined, dried over anhydrous sodium sulfate, filtered and concentrated to afford the crude product which when necessary was purified by column chromatography.

General Reductive Amination Procedure. To a solution of the amine in DCM (0.1 M) was added the aldehyde (1.1 eq) and stirred at room temperature for 30 minutes. Then sodium triacetoxyborohydride (1.5 eq) was added as one portion and the reaction was tracked by LCMS. The reaction was usually complete within 5 hours. Upon completion the mixture was diluted with brine and basified with 10% NaOH. The layers were separated and the aqueous layer extracted with DCM (3 times). The organic layers were combined, dried over anhydrous sodium sulfate, filtered and concentrated to afford the crude product which was purified by column chromatography.

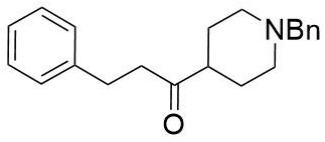

*1-(1-benzylpiperidin-4-yl)-3-phenylpropan-1-one (**5**)*. Methyl 1-benzylpiperidine-4-carboxylate **4** (0.50 g, 2.1 mmol) as a solution in THF (43 mL, 0.05 M) was added to a flame dried 250 mL round bottom flask containing the Weinreb amine salt (0.26 g, 2.7 mmol, 1.25 eq) and stirred at -5 °C. Phenethylmagnesium chloride (8.6 mL, 8.6 mmol, 4.0 eq) was then added dropwise and the reaction was allowed to stir until complete consumption of starting material at -5 °C. After formation of the Weinreb amide the reaction was slowly warmed to room temperature and tracked by LCMS. After an additional 2 hours of stirring at room temperature the reaction was quenched with NH_4Cl (20 mL) and basified with 10% NaOH. The mixture was further partitioned with EtOAc and separated. The aqueous layer was extracted with DCM (3 times). The organic layers were combined, dried over anhydrous magnesium sulfate, filtered and concentrated to afford 1-(1-benzylpiperidin-4-yl)-3-phenylpropan-1-one (0.630 g, 96% yield). ^{1}H NMR (400 MHz, $CDCl_3$) δ 7.34 – 7.29 (m, 4H), 7.29 – 7.21 (m, 3H), 7.21 – 7.15 (m, 3H), 3.48 (s, 2H), 2.94 – 2.82 (m, 4H), 2.80 – 2.71 (m, 2H), 2.26 (tt, *J* = 11.5, 4.0 Hz, 1H), 1.98 (tt, *J* = 11.6, 6.6 Hz, 2H), 1.80 – 1.73 (m, 2H), 1.65 (dtd, *J* = 13.1, 11.5, 3.7 Hz, 2H). ^{13}C NMR (100 MHz, $CDCl_3$) δ 212.28, 141.50, 138.54, 129.30, 128.70, 128.56, 128.43, 127.22, 126.30,

63.43, 53.29, 49.19, 42.29, 29.88, 27.97. HRMS calc'd for $C_{21}H_{26}ON$ 308.2009; found [M+H] 308.2004.

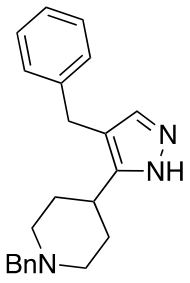

*1-benzyl-4-(4-benzyl-1H-pyrazol-3-yl)piperidine (**6**)*. To a solution of 1-(1-benzylpiperidin-4-yl)-3-phenylpropan-1-one 5 (0.45 g, 1.5 mmol) in THF (15 mL, 0.1 M) in a flame dried 100 mL round bottom flask was added NaH (0.21 g, 8.8 mmol, 6 eq) and stirred at RT. Methyl formate (1.76 g, 29 mmol, 20 eq) was then added followed by 15-crown-5 (0.16 g, 73 mmol, 0.5 eq). The reaction was tracked by LCMS and after 1 hour was quenched with 1.0 mL of H_2O dropwise. The reaction was then diluted with MeOH (15 mL, 0.1 M) followed by the dropwise addition of hydrazine (0.7 g, 22 mmol, 15 eq) and tracked by LCMS. After an additional hour of stirring the reaction was concentrated *in vacuo* to remove MeOH. The oily residue was partitioned between water and DCM and basified with 10% NaOH solution. The layers were separated and the aqueous layer was extracted with DCM (3 times). The organic layers were combined, dried over anhydrous magnesium sulfate, filtered and concentrated. The crude mixture was then purified on a 12 gram combiflash column with a gradient from 0-70% DCM:MeOH:NH_4OH (90:10:0.5) in DCM to afford 1-benzyl-4-(4-benzyl-1H-pyrazol-3-yl)piperidine (0.24 g, 48% yield). Scaleup: Conducted as described above with minor variations to equivalents: NaH (4.5 eq), 15-crown-5 (0.25 eq), MeOH (0.33 M), hydrazine (10 eq) (2.51 g, 35% yield). ^{1}H NMR (600 MHz, $CDCl_3$) δ 7.32 – 7.21 (m, 8H), 7.18 – 7.13 (m, 2H), 3.79 (s, 2H), 3.67 (s, 1H), 3.50 (s, 2H), 2.94 (dt, *J* = 11.3, 2.9 Hz, 2H), 2.66 – 2.56 (m, 1H), 1.99 (tt, *J* = 11.7, 1.5 Hz, 2H), 1.89 – 1.80 (m, 2H), 1.75 – 1.67 (m, 2H). ^{13}C NMR (150 MHz, $CDCl_3$) δ 161.70, 141.37, 138.29, 129.49, 128.58, 128.41, 127.27, 126.18, 116.00, 70.74, 63.60, 54.14, 31.84, 30.03. HRMS calc'd for $C_{22}H_{26}N_3$ 332.21212; found [M+H] 332.21145. LCMS 75-95% 3 minutes MeOH:H_2O gradient >95% pure rt = 0.620.

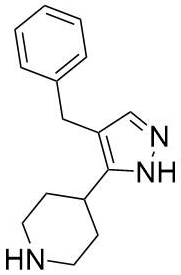

*4-(4-benzyl-1H-pyrazol-3-yl)piperidine (**3**)*. Prepared by general hydrogenation procedure B from **6**. Material filtered through celite to remove the Pd/C, concentrated, and then taken on to the next step crude. Analytical sample purified for MAGI assay on a 12 gram combiflash column with a gradient from 0-70% DCM:MeOH:NH_4OH (90:10:0.5) in DCM to afford 4-(4-benzyl-1H-pyrazol-3-yl)piperidine. ^{1}H NMR (400 MHz, $CDCl_3$) δ 7.30 (s, 1H), 7.27 – 7.20 (m, 2H), 7.18 – 7.08 (m, 3H), 3.77 (s, 2H), 3.41 (dt, *J* = 12.8, 3.0 Hz, 2H), 2.91 (td, *J* = 13.1, 3.2 Hz, 2H), 2.81 (tt, *J* = 11.7, 3.8 Hz, 1H), 2.02 – 1.91 (m, 2H), 1.85 – 1.74 (m, 2H). ^{13}C NMR (100 MHz, $CDCl_3$) δ 177.14, 149.03, 140.68, 131.58, 128.74, 128.52, 126.51, 116.92, 43.99, 31.80, 31.23, 29.91, 28.64. HRMS calc'd for $C_{15}H_{20}N_3$ 242.16517; found [M+H] 242.16551. LCMS 75-95% 3 minutes MeOH:H_2O gradient >95% pure rt = 0.581.

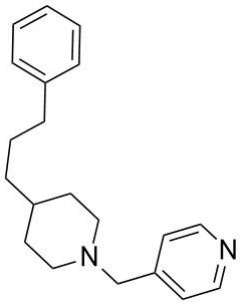

*4-((4-(3-phenylpropyl)piperidin-1-yl)methyl)pyridine (**2**)*. Prepared by Anthony Prosser. Prepared by general reductive amination procedure from 4-(3-phenylpropyl)piperidine. Purified on a 4 gram combiflash column with a gradient of 0-40% DCM:MeOH:NH_4OH (90:10:0.5) in DCM to afford 4-((4-(3-phenylpropyl)piperidin-1-yl)methyl)pyridine (0.045 g, 62% yield). ^1H NMR (400 MHz, $CDCl_3$) δ 8.54 – 8.50 (m, 2H), 7.32 – 7.23 (m, 4H), 7.22 – 7.13 (m, 3H), 3.47 (s, 2H), 2.85 – 2.77 (m, 2H), 2.62 – 2.55 (m, 2H), 1.95 (t, *J* = 2.0 Hz, 2H), 1.71 – 1.57 (m, 4H), 1.33 – 1.18 (m, 5H). ^{13}C NMR (100 MHz, $CDCl_3$) δ 149.65, 148.10, 142.68, 128.34, 125.62, 123.89, 62.18, 54.11, 36.20, 36.14, 35.51, 32.32, 28.72. LCMS 25-95% 8 minutes MeOH:H_2O gradient >95% pure rt = 6.248.

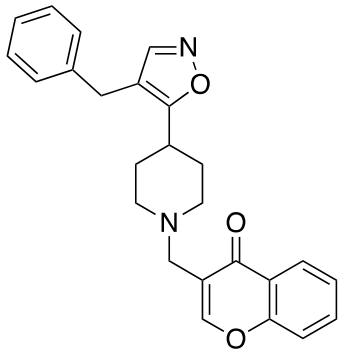

*3-((4-(4-benzyl-1H-pyrazol-5-yl)piperidin-1-yl)methyl)-4H-chromen-4-one (**8**)*. Compound **8** was prepared by general reductive amination procedure from **3**. To a solution of 4-(4-benzyl-1H-pyrazol-3-yl)piperidine acetate salt (0.162 g, 0.537 mmol) in DCM was added 4-oxo-4H-chromene-3-carbaldehyde (0.208 g, 0.972 mmol) and stirred at RT. Sodium triacetoxyborohydride (0.305 g, 1.43 mmol) was then added. The reaction was tracked by LCMS until completion. Products were purified with brine and basified with 10% NaOH solution. The layers were separated and the aqueous layer was extracted with DCM (3 times). The organic layers were combined, dried over anhydrous sodium sulfate, filtered, and concentrated. The crude mixture was then purified on a 4 gram column with a gradient from 0-70% DCM:MeOH:NH_4OH (9:1:0.5) in DCM to afford 3-((4-(4-benzyl-1H-pyrazol-5-yl)piperidin-1-yl)methyl)-4H-chromen-4-one (0.113 g, 53%). ^1H NMR (400 MHz, $CDCl_3$) δ 8.27 – 8.17 (m, 1H), 8.02 (t, *J* = 0.8 Hz, 1H), 7.71 – 7.60 (m, 1H), 7.51 – 7.42 (m, 1H), 7.42 – 7.34 (m, 1H), 7.32 (s, 1H), 7.26 (tt, *J* = 7.0, 0.9 Hz, 3H), 7.18 (dd, *J* = 7.7, 1.8 Hz, 1H), 7.17 – 7.12 (m, 2H), 3.81 (s, 2H), 3.49 (d, *J* = 1.0 Hz, 2H), 3.02 (dt, *J* = 11.9, 3.1 Hz, 2H), 2.64 (tt, *J* = 12.1, 3.9 Hz, 1H), 2.15 (td, *J* = 11.9, 2.4 Hz, 2H), 1.90 (qd, *J* = 12.5, 3.7 Hz, 2H), 1.80 – 1.74 (d, 2H); ^{13}C NMR (100 MHz, $CDCl_3$) δ 177.76, 156.38, 154.84, 141.12, 133.50, 128.36, 128.35, 125.95, 125.86, 125.06, 123.84, 120.40, 118.10, 115.84, 77.25, 53.99, 52.66, 33.22, 31.66, 29.81. HRMS calculated for $C_{25}H_{26}O_2N_3$ 400.2025; found [M+H] 400.2016. LCMS 25-95% 8 minutes MeOH:H_2O gradient >95% pure rt= 6.751. LCMS 75-95% 3 minutes MeOH: H_2O gradient >95% pure rt= 0.889.

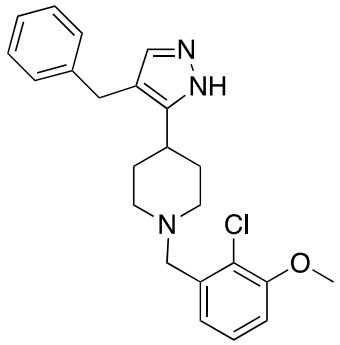

*4-(4-benzyl-1H-pyrazol-5-yl)-1-(2-chloro-3-methoxybenzyl)piperidine (**9**)*. Compound **9** was prepared by a general reductive amination procedure from **3**. To a solution of 4-(4-benzyl-1H-pyrazol-3-yl)piperidine acetate salt (0.162 g, 0.537 mmol) in DCM was added 2-chloro-3methoxybenzaldehyde (0.316 g, 1.85 mmol) and stirred at room temperature for 30 min. To the reaction, sodium triacetoxyborohydride (0.480 g, 2.27 mmol) was added in one portion. Progression of the reaction was monitored by LCMS until completion. The mixture was diluted with brine and basified with 10% NaOH solution. The layers were separated and the aqueous layer was extracted with DCM (3 times). The organic layers were combined, dried over anhydrous sodium sulfate, filtered, and concentrated. The crude product was purified on a 12 gram silica column with a gradient from 0-70% DCM:MeOH:NH_4OH (9:1:0.5) in DCM to afford 4-(4-benzyl-1H-pyrazol-5-yl)-1-(2-chloro-3-methoxybenzyl)piperidine (0.0950 g, 45% yield). ^{1}H NMR (400 MHz, $CDCl_3$) δ 7.28 (s, 1H), 7.27 (m, 1H), 7.25 (m, 1H), 7.21-7.14 (m, 4H), 7.12 (dd, *J* = 1.6, 7.8 Hz, 1H), 6.83 (dd, *J* = 1.4, 8.2 Hz, 1H), 3.89 (s, 3H), 3.81 (s, 2H), 3.64 (s, 2H), 2.98 (d, *J* = 11.2 Hz, 2H), δ 2.64 (tt, *J* = 4.0, 12.0 Hz, 1H), 2.13 (td, *J* = 2.56, 11.7 Hz, 2H), 1.82 (qd, *J* = 3.6, 8.8, 12.4 Hz, 2H) 1.73 (d, *J* = 10.4 Hz, 2H); ^{13}C NMR (100 MHz, $CDCl_3$) δ 155.15, 141.18, 128.52, 126.86, 126.14, 122.48, 110.38, 59.72, 56.34, 33.55, 31.85, 29.95, 14.09. HRMS calc'd for $C_{23}H_{27}ClN_3O$ 396.1843; found [M+H] 396.1842. LCMS 25-95% 8 minutes MeOH:H_2O gradient >95% pure rt = 6.695. LCMS 75-95% 3 minutes MeOH: H_2O gradient >95% pure rt =1.005.

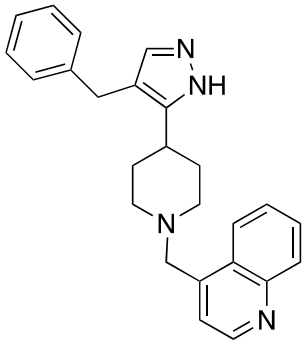

*4-((4-(4-benzyl-1H-pyrazol-5-yl)piperidin-1-yl)methyl)quinoline (**10**)*. Compound **10** was prepared by general reductive amination procedure from **3**. To a solution of 4-(4-benzyl-1H-pyrazol-3-yl)piperidine acetate salt (0.162 g, 0.537 mmol) in DCM was added quinoline-4-carbaldehyde (0.270 g, 1.72 mmol) and stirred at RT. Approximately 5 drops of acetic acid was added and the solution was allowed to stir for 30 min. Sodium triacetoxyborohydride (0.286 g, 1.35 mmol) was then added in one portion to the solution. The reaction was monitored by LCMS until completion. The reaction was diluted with brine and basified with 10% NaOH solution. The layers were separated and the aqueous layer was extracted with DCM (3 times). The organic layers were combined, dried over anhydrous sodium sulfate, filtered, and concentrated. The crude mixture was then purified on a 12 gram silica column with a gradient from 0-70% DCM:MeOH:NH_4OH (9:1:0.5) in DCM to afford 4-((4-(4-benzyl-1H-pyrazol-5-yl)piperidin-1-yl)methyl)quinoline (0.136 g, 66%). ^{1}H NMR (400 MHz, $CDCl_3$) δ 8.84 (d, 1H), 8.23 (d, 1H), 8.13 (d, 1H), 7.71-7.67 (m, 1H), 7.55-7.51 (m, 1H), 7.44 (d,

1H), 7.29-7.24 (m, 2H), 7.21-7.15 (m, 3H), 3.93 (s, 2H), 3.81 (s, 2H), 2.99 (d, 2H), 2.70-2.62 (tt, 1H), 2.19-2.13 (t, 2H), 1.94-1.84 (m, 2H), 1.76 (d, 2H); ^{13}C NMR (100 MHz, $CDCl_3$) δ 150.12, 148.27, 144.41, 141.02, 129.88, 129.10, 129.36, 128.36, 128.37, 127.66, 126.25, 126.01, 124.12, 121.11, 116.03, 59.80, 54.44, 53.43, 33.49, 31.74, 2.81. HRMS calculated for $C_{25}H_{27}N_4$ 383.2236; found [M+H] 383.2235. LCMS 25-95% 8 minutes MeOH:H_2O gradient >95% pure rt= 6.207. LCMS 75-95% 3 minutes MeOH: H_2O gradient >95% pure rt= 0.872.

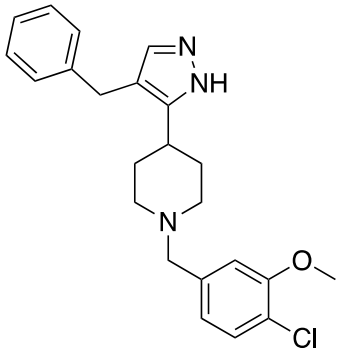

*4-(4-benzyl-1H-pyrazol-5-yl)-1-(4-chloro-3-methoxybenzyl)piperidine (**11**)*. Compound **11** was prepared by general reductive amination procedure from **3**. To a solution of 4-(4-benzyl-1H-pyrazol-3-yl)piperidine acetate salt (0.162 g, 0.537 mmol) in DCM was added 4-chloro-3methoxybenzaldehyde (0.337 g, 1.98 mmol) and stirred at room temperature for 30 min. To the reaction, sodium triacetoxyborohydride (0.507 g, 2.39 mmol) was added in one portion. Progression of the reaction was monitored by LCMS until completion. The mixture was diluted with brine and basified with 10% NaOH solution. The layers were separated and the aqueous layer was extracted with DCM (3 times). The organic layers were combined, dried over anhydrous sodium sulfate, filtered, and concentrated. The crude product was purified on a 12 gram silica column with a gradient from 0-70% DCM:MeOH:NH_4OH (9:1:0.5) in DCM to afford 4-(4-benzyl-1H-pyrazol-5-yl)-1-(4-chloro-3-methoxybenzyl)piperidine (0.139 g, 65% yield). ^{1}H NMR (400 MHz, $CDCl_3$) δ 7.33 – 7.11 (m, 7H), 6.95 (d, *J* = 1.9 Hz, 1H), 6.82 (dd, *J* = 8.0, 1.8 Hz, 1H), 3.83 (d, *J* = 19.8 Hz, 5H), 3.47 (d, *J* = 3.8 Hz, 2H), 2.93 (dt, *J* = 11.7, 3.2 Hz, 2H), 2.62 (tt, *J* = 11.8, 4.0 Hz, 1H), 2.00 (td, *J* = 11.6, 2.5 Hz, 2H), 1.92 – 1.72 (m, 4H); ^{13}C NMR (100 MHz, $CDCl_3$) δ 154.81, 141.03, 138.67, 129.68, 128.38, 128.34, 126.01, 121.75, 120.76, 115.98, 112.57, 62.89, 56.07, 53.95, 53.44, 33.47, 31.61, 29.80. HRMS calculated for $C_{23}H_{27}ON_3Cl$ 396.1843; found [M+H] 396.1850. LCMS 25-95% 8 minutes MeOH:H_2O gradient >95% pure rt= 7.137. LCMS 75-95% 3 minutes MeOH: H_2O gradient >95% pure rt=1.108.

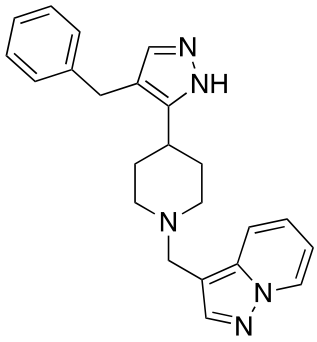

*3-((4-(4-benzyl-1H-pyrazol-5-yl)piperidin-1-yl)methyl)pyrazolo[1,5-a]pyridine (**12**)*. Compound **12** was prepared by general reductive amination procedure from **3**. To a solution of 4-(4-benzyl-1H-pyrazol-3-yl)piperidine acetate salt (0.150 g, 0.498 mmol) in DCM was added pyrazolo[1,5-a]pyridine-3-carbaldehyde (0.111 g, 0.760 mmol) and stirred at room temperature for 30 min. To the reaction, sodium triacetoxyborohydride (0.190 g, 0.897 mmol) was added in one portion. Progression of the reaction was monitored by LCMS until

completion. The mixture was diluted with brine and basified with 10% NaOH solution. The layers were separated and the aqueous layer was extracted with DCM (3 times). The organic layers were combined, dried over anhydrous sodium sulfate, filtered, and concentrated. The crude product was purified on a 12 gram silica column with a gradient from 0-70% DCM:MeOH:NH_4OH (9:1:0.5) in DCM to afford 3-((4-(4-benzyl-1H-pyrazol-5-yl)piperidin-1-yl)methyl)pyrazolo[1,5-a]pyridine (0.0719 g, 39% yield). ^{1}H NMR (400 MHz, $CDCl_3$) δ 7.96 (t, J = 2.1 Hz, 1H), 7.47 (d, *J* = 8.8 Hz, 1H), 7.32 – 7.06 (m, 7H), 6.96 (d, *J* = 6.6 Hz, 1H), 6.55 (t, *J* = 2.1 Hz, 1H), 4.07 (s, 2H), 3.83 (d, *J* = 1.9 Hz, 2H), 3.12 (d, *J* = 10.9 Hz, 2H), 2.75 – 2.59 (m, 1H), 2.29 (t, *J* = 11.4 Hz, 2H), 1.96 (q, *J* = 12.2 Hz, 2H), 1.26 (d, *J* = 5.9 Hz, 1H); ^{13}C NMR (100 MHz, $CDCl_3$) δ 141.10, 141.05, 140.66, 138.48, 128.38, 126.00, 123.25, 116.06, 109.93, 96.90, 57.06, 54.81, 53.45, 33.33, 31.80, 29.81. HRMS calculated for $C_{23}H_{26}N_5$ 372.2188; found [M+H] 372.2192. LCMS 25-95% 8 minutes MeOH:H_2O gradient >95% pure rt= 6.245. LCMS 75-95% 3 minutes MeOH: H_2O gradient >95% pure rt= 0.798.

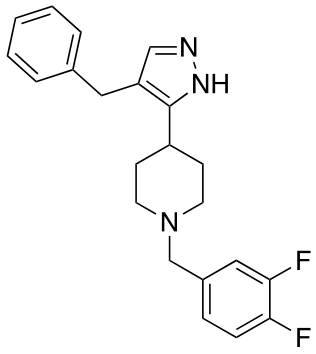

*4-(4-benzyl-3H-pyrazol-5-yl)-1-(3,4-difluorobenzyl)piperidine (**13**)*. Compound **13** was prepared by general reductive amination procedure from **3**. To a solution of 4-(4-benzyl-1H-pyrazol-3-yl)piperidine acetate salt (0.182 g, 0.604 mmol) in DCM was added 3,4-difluorobenzaldehyde (0.155 g, 1.09 mmol) and stirred at RT. Sodium triacetoxyborohydride (0.249 g, 1.95 mmol) was then added. Progression of the reaction was monitored by LCMS until completion. The mixture was diluted with brine and basified with 10% NaOH solution. The layers were separated and the aqueous layer was extracted with DCM (3 times). The organic layers were combined, dried over anhydrous sodium sulfate, filtered, and concentrated. The crude product was purified on a 12 gram silica column with a gradient from 0-70% DCM:MeOH:NH_4OH (9:1:0.5) in DCM to afford 4-(4-benzyl-3H-pyrazol-5-yl)-1-(3,4-difluorobenzyl)piperidine (0.0941 g, 42%). ^{1}H NMR (400 MHz, $CDCl_3$) δ 7.36 (s, 1H), 7.32 – 7.23 (m, 2H), 7.22 – 7.12 (m, 4H), 7.08 – 6.97 (m, 2H), 3.84 (s, 2H), 3.44 (s, 2H), 2.91 (dt, *J* = 11.8, 3.1 Hz, 2H), 2.64 (tt, *J* = 11.9, 3.9 Hz, 1H), 2.01 (td, *J* = 11.6, 2.3 Hz, 2H), 1.94 – 1.82 (m, 2H), 1.78 – 1.68 (m, 2H), 1.36 – 1.16 (m, 1H); ^{13}C NMR (100 MHz, $CDCl_3$) δ 151.59, 150.74, 141.26, 135.81, 135.77, 135.72, 128.46, 126.08, 124.75, 124.72, 124.69, 124.66, 117.75, 117.58, 116.95, 116.78, 115.88, 68.08, 62.25, 33.51, 31.76, 29.91, 22.77, 14.25; ^{19}F NMR (376 MHz, $CDCl_3$) δ -143.08, -145.33. HRMS calculated for $C_{22}H_{24}N_3F_2$ 368.1938; found [M+H] 368.1932. LCMS 25-95% 8 minutes MeOH:H_2O gradient >95% pure rt= 6.563. LCMS 75-95% 3 minutes MeOH: H_2O gradient >95% pure rt= 0.821.

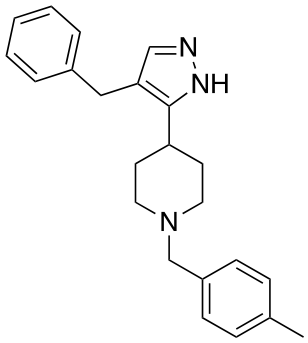

*4-(4-benzyl-1H-pyrazol-5-yl)-1-(4-methylbenzyl)piperidine (**14**)*. Compound **14** was prepared by general reductive amination procedure from **3**. To a solution of 4-(4-benzyl-1H-pyrazol-3-yl)piperidine acetate salt (0.166 g, 0.551 mmol) in DCM was added 4-methylbenzaldehyde (0.947 g, 7.88 mmol) and stirred at room temperature for 30 min. To the reaction, sodium triacetoxyborohydride (0.227 g, 1.07 mmol) was added in one portion. Progression of the reaction was monitored by LCMS until completion. The mixture was diluted with brine and basified with 10% NaOH solution. The layers were separated and the aqueous layer was extracted with DCM (3 times). The organic layers were combined, dried over anhydrous sodium sulfate, filtered, and concentrated. The crude product was purified on a 12 gram silica column with a gradient from 0-70% DCM:MeOH:NH_4OH (9:1:0.5) in DCM to afford 4-(4-benzyl-1H-pyrazol-5-yl)-1-(4-methylbenzyl)piperidine (0.147 g, 77% yield). ^{1}H NMR (400 MHz, $CDCl_3$) δ 7.34 – 7.07 (m, 10H), 3.81 (s, 2H), 3.49 (s, 2H), 2.96 (dt, *J* = 12.0, 3.3 Hz, 2H), 2.62 (tt, *J* = 11.8, 4.1 Hz, 1H), 2.33 (s, 3H), 2.00 (td, *J* = 11.6, 2.6 Hz, 2H), 1.91 – 1.76 (m, 2H), 1.72 (d, *J* = 3.6 Hz, 1H); ^{13}C NMR (100 MHz, $CDCl_3$) δ 141.07, 136.63, 129.23, 128.87, 128.36, 125.97, 115.87, 63.05, 33.39, 31.61, 29.79, 21.11. HRMS calculated for $C_{23}H_{28}N_3$ 346.2283; found [M+H] 346.2283. LCMS 25-95% 8 minutes MeOH:H_2O gradient >95% pure rt= 6.862. LCMS 75-95% 3 minutes MeOH: H_2O gradient >95% pure rt= 0.898. LCMS 95% ISO 3 minutes MeOH: H_2O gradient >95% pure rt= 0.907.

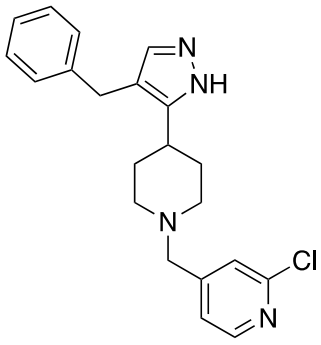

*4-((4-(4-benzyl-1H-pyrazol-3-yl)piperidin-1-yl)methyl)-2-chloropyridine (**15**)*. Developed by Anthony Prosser. Prepared by general reductive amination procedure from **3**. Purified on a 12 gram combiflash column with a gradient of 0-70% DCM:MeOH:NH4OH (90:10:0.5) in DCM to afford 4-((4-(4-benzyl-1H-pyrazol-3-yl)piperidin-1-yl)methyl)-2-chloropyridine (145 mg, 60% yield over two steps). ^{1}H NMR (400 MHz, $CDCl_3$) δ 8.50 (s, 1H), 8.37 (d, *J* = 4.9 Hz, 1H), 7.48 – 7.42 (m, 1H), 7.35 (s, 1H), 7.24 (tt, *J* = 6.5, 1.1 Hz, 2H), 7.19 – 7.11 (m, 3H), 3.82 (s, 2H), 3.58 (s, 2H), 2.90 (dt, *J* = 11.7, 3.1 Hz, 2H), 2.64 (tt, *J* = 12.1, 3.9 Hz, 1H), 2.14 (td, *J* = 11.8, 2.4 Hz, 2H), 1.99 – 1.83 (m, 2H), 1.78 – 1.69 (m, 2H). ^{13}C NMR (100 MHz, $CDCl_3$) δ 149.10, 147.62, 145.69, 141.05, 131.76, 128.36, 128.33, 126.01, 124.23, 115.89, 58.50, 54.28, 33.28, 31.76, 29.81. HRMS calc'd for $C_{21}H_{24}N_4Cl$ 367.16840; found [M+H] 367.16865. LCMS 75-95% 3 minutes MeOH:H_2O gradient >95% pure rt = 0.665. LCMS 25-95% 8 minutes MeOH:H_2O gradient >95% pure rt = 5.457.

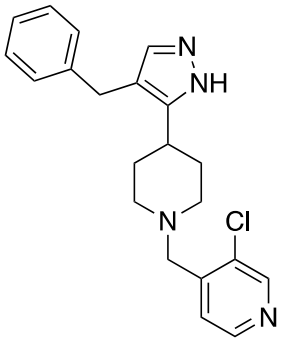

*4-((4-(4-benzyl-1H-pyrazol-3-yl)piperidin-1-yl)methyl)-3-chloropyridine (**16**)*. Developed by Anthony Prosser. Prepared by general reductive amination procedure from material **3**. Purified on a 12 gram combiflash column with a gradient of 0-70% DCM:MeOH:NH_4OH (90:10:0.5) in DCM to afford 4-((4-(4-benzyl-1H-pyrazol-3-yl)piperidin-1-yl)methyl)-3-chloropyridine (155 mg, 64% yield over two steps). ^{1}H NMR (400 MHz, $CDCl_3$) δ 8.24 (d, *J* = 5.0 Hz, 1H), 7.35 (s, 1H), 7.28 (s, 1H), 7.28 – 7.21 (m, 2H), 7.19 – 7.12 (m, 4H), 3.82 (s, 2H), 3.45 (s, 2H), 2.85 (dt, *J* = 11.6, 3.0 Hz, 2H), 2.62 (tt, *J* = 11.9, 3.9 Hz, 1H), 2.04 (td, *J* = 11.7, 2.4 Hz, 2H), 1.88 (qd, *J* = 12.3, 3.6 Hz, 2H), 1.78 – 1.67 (m, 2H). ^{13}C NMR (100 MHz, $CDCl_3$) δ 151.83, 149.47, 148.59, 141.06, 134.61, 128.34, 126.00, 123.95, 122.44, 115.87, 61.45, 54.13, 33.31, 31.64, 29.82. HRMS calc'd for $C_{21}H_{24}N_4Cl$ 367.16840; found [M+H] 367.16849. LCMS 75-95% 3 minutes MeOH:H_2O gradient >95% pure rt = 0.680. LCMS 25-95% 8 minutes MeOH:H_2O gradient >95% pure rt = 5.672.

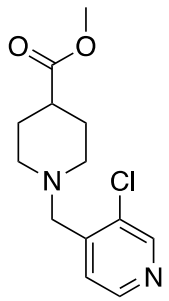

*Methyl 1-((3-chloropyridin-4-yl)methyl)piperidine-4-carboxylate (**18**)*. Prepared by general reductive amination procedure from methyl 4-piperidinecarboxylate **17**. To a solution of methyl 4-piperidinecarboxylate salt (3.37 g, 23.6 mmol) in DCM was added 3-chloroisonicotinaldehyde (4.00 g, 28.3 mmol) and stirred at room temperature for 30 min. To the reaction, sodium triacetoxyborohydride (7.49 g, 35.3 mmol) was added in one portion. Progression of the reaction was monitored by LCMS until completion. The mixture was diluted with brine and basified with 10% NaOH solution. The layers were separated and the aqueous layer was extracted with DCM (3 times). The organic layers were combined, dried over anhydrous sodium sulfate, filtered, and concentrated. The crude product was purified on a 24 gram silica column with a gradient from 0-70% DCM:MeOH:NH_4OH (9:1:0.5) in DCM to afford methyl 1-((3-chloropyridin-4-yl)methyl)piperidine-4-carboxylate (3.68 g, 58% yield). ^{1}H NMR (400 MHz, $CDCl_3$) δ 8.49 (s, 1H), 8.40 (d, *J* = 5.0 Hz, 1H), 7.45 (d, *J* = 5.0 Hz, 1H), 3.65 (s, 3H), 3.51 (s, 2H), 2.82 – 2.72 (m, 2H), 2.27 (ttd, *J* = 11.0, 4.0, 2.4 Hz, 1H), 2.10 (td, *J* = 11.4, 2.6 Hz, 2H), 1.89 – 1.66 (m, 2H), 1.18 (tq, *J* = 7.1, 1.3 Hz, 2H).

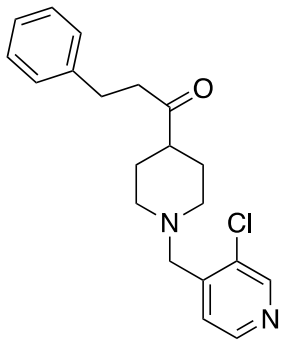

*1-(1-((3-chloropyridin-4-yl)methyl)piperidin-4-yl)-3-phenylpropan-1-one (**19**)*. Methyl 1-((3-chloropyridin-4-yl)methyl)piperidine-4-carboxylate **18** (0.919 g, 3.42 mmol) as a solution in THF (0.1 M) was added to a flame dried 100 mL round bottom flask containing the Weinreb amine salt (0.420 g, 1.26 mmol, 1.2 eq) and stirred at 0 °C. Phenethylmagnesium chloride (19.5 mL, 3.2 mmol, 4.5 eq) was then added dropwise and the reaction was allowed to stir until complete

consumption of starting material at 0 °C. After formation of the Weinreb amide the reaction was slowly warmed to room temperature and tracked by LCMS. After an additional 2 hours of stirring at room temperature the reaction was quenched with NH_4Cl (20 mL) and basified with 10% NaOH. The mixture was further partitioned with EtOAc and separated. The aqueous layer was extracted with DCM (3 times). The organic layers were combined, dried over anhydrous magnesium sulfate, filtered and concentrated to afford 1-(1-((3-chloropyridin-4-yl)methyl)piperidin-4-yl)-3-phenylpropan-1-one (0.185 g, 16% yield).

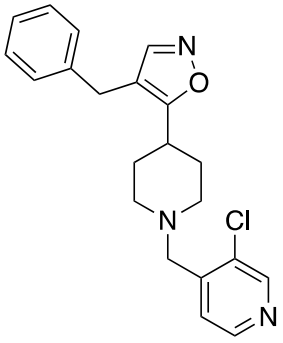

*4-benzyl-5-(1-((3-chloropyridin-4-yl)methyl)piperidin-4-yl)isoxazole (**21**)*. To a solution of 1-(1-((3-chloropyridin-4-yl)methyl)piperidin-4-yl)-3-phenylpropan-1-one 19 (0.185 g, 0.540 mmol) in THF (12 mL, 0.1 M) in a flame dried 100 mL round bottom flask was added NaH (0.0580 g, 2.43 mmol, 4.5 eq) and stirred at RT. Methyl formate (0.648 g, 10.8 mmol, 20 eq) was then added followed by the addition of 5 mL of dry MeOH. The reaction was tracked by LCMS and after 1 hour was quenched with 5 mL of H_2O dropwise. To the reaction (0.516 g, 1.51 mmol) was added hydroxylamine hydrochloride (0.209 g, 3.01 mmol, 2 eq) and the reaction was tracked by LCMS. After an additional hour the reaction was partitioned between water and EtOAc, and then basified with 10% NaOH solution. The layers were separated and the aqueous layer was extracted with DCM (3 times). The organic layers were combined, dried over anhydrous sodium sulfate, filtered, and concentrated. The oily residue was subjected to acetic acid (15 mL, 0.1 M) at 75 °C. The reaction was tracked with LCMS and allowed to run overnight to drive the cyclization to completion. The crude product was concentrated and purified on a 24 gram silica column with a gradient from 0-70% DCM:MeOH:NH_4OH (9:1:0.5) in DCM to afford 4-benzyl-5-(1-((3-chloropyridin-4-yl)methyl)piperidin-4-yl)isoxazole (0.254 g, 49%). ^{1}H NMR (400 MHz, $CDCl_3$) δ 8.51 (s, 1H), 8.44 (d, *J* = 5.0 Hz, 1H), 7.97 (s, 1H), 7.50 (d, *J* = 4.9 Hz, 1H), 7.38 – 7.07 (m, 5H), 3.75 (s, 2H), 3.61 (s, 2H), 2.98 – 2.84 (m, 2H), 2.78 (tt, *J* = 11.8, 3.9 Hz, 1H), 2.17 (td, *J* = 11.7, 2.2 Hz, 2H), 2.15 – 1.99 (m, 2H), 1.83 – 1.63 (m, 2H); ^{13}C NMR (100 MHz, $CDCl_3$) δ 170.36, 151.67, 148.98, 147.57, 145.54, 139.10, 131.75, 128.70, 128.15, 126.61, 124.28, 112.09, 79.95, 58.28, 53.45, 33.73, 30.09, 28.43; HRMS calculated for $C_{21}H_{23}ON_3Cl$ 368.1535; found [M+H] 368.1523. LCMS 25-95% 8 minutes MeOH:H_2O gradient >95% pure rt= 3.862. LCMS 75-95% 3 minutes MeOH: H_2O gradient >95% pure rt= 0.617.

References

1. Bawkar, S.; Kamble, A. *HIV Drug Market by Medication class [multi-class combination drugs, nucleoside reverse transcriptase inhibitors (NRTIs), non-nucleoside reverse transcriptase inhibitors (NNRTIs), protease inhibitors (PIs), fusion inhibitors (FI), entry inhibitors, and HIV integrase stand transfer inhibitors] - Global Opportunity Analysis and Industry Forecast, 2014-2022*; Allied Market Research: 2017.

2. AVERT, HIV AND AIDS IN THE UNITED STATES OF AMERICA (USA). **2017,** *2017*.

3. CDC. Vital Signs: HIV Diagnosis, Care, and Treatment Among Persons Living with HIV — United States, 2011. MMWR 2014; 63 (Early Release):1-6.

4. Debnath, B.; Xu, S.; Grande, F.; Garofalo, A.; Neamati, N., Small molecule inhibitors of CXCR4. *Theranostics* **2013,** *3* (1), 47-75.

5. Henrich, T. J.; Kuritzkes, D. R., HIV-1 entry inhibitors: recent development and clinical use. *Curr. Op. Virol.* **2013,** *3* (1), 51-57.

6. Kalinina, O. V.; Pfeifer, N.; Lengauer, T., Modelling binding between CCR5 and CXCR4 receptors and their ligands suggests the surface electrostatic potential of the co-receptor to be a key player in the HIV-1 tropism. *Retrovirology* **2013,** *10* (1), 130.

7. Alkhatib, G., The biology of CCR5 and CXCR4. *Curr Op. HIV AIDS.* **2009,** *4* (2), 96.

8. De Clercq, E., The bicyclam AMD3100 story. *Nat. Rev. Drug Discov.*, **2003***, 2*, 581-587.

9. Fuzeon: Indications and Dosage. *RxList* **2015**.

10. Esté, J. A.; Telenti, A., HIV entry inhibitors. *The Lancet* **2007,** *370* (9581), 81-88.

11. NIH, AIDSinfo Drug Database. NIH.gov: 2016.

12. Wilson, L. J.; Liotta, D. C., Emergence of small-molecule CXCR4 antagonists as novel immune and hematopoietic system regulatory agents. *Drug Develop. Res.* **2011**, *72*, 598–602.

13. Moyle, G.; DeJesus, E.; Boffito, M.; Wong, R. S.; Gibney, C.; Badel, K.; MacFarland, R.; Calandra, G.; Bridger, G.; Becker, S., Proof of activity with AMD11070, an orally bioavailable inhibitor of CXCR4-tropic HIV type 1. *Clin. Infect. Dis.* **2009,** *48* (6), 798-805.

14. Clark, M.; Gohil, K., In the Crowded HIV Market, There's Room for Innovation. *P T.* **2015,** *40* (5), 364-365.

15. Chaudhari, K., Diagnostics and Therapeutics for HIV: Global Markets. *BCC Research*: Wellesley, MA, 2014; Vol. PHM058B, p 1-196.

16. Consolidated guidelines on the use of antiretroviral drugs for treating and preventing HIV infection: recommendations for a public health approach. *World Health Organization*: 2016; p 1-480.

17. Consolidated guidelines on the use of antiretroviral drugs for treating and preventing HIV infection*. World Health Organization*: 2013; p 1-272.

18. Cha, A. E. Groundbreaking guidelines expand population on HIV drugs by millions. But who will pay? *Washington Post: To Your Health* [Online], 2015.

19. U.S. Federal Funding for HIV/AIDS: Trends Over Time. *Kaiser Family Foundation Fact Sheets* [Online], 2016, p. 1-4.

20. Lehr, P., *Global Markets for Infectious Disease Treatments*. BCC Research: Wellesley, MA, 2016; Vol. PHM061C.

21. Hudson, J., Generic take-up in the pharmaceutical market following patent expiry: a multi-country study. *Int. Rev.Law Econ.* **2000,** *20* (2), 205-221.

22. Bedell, T. A.; Hone, G. A.; Du Bois, J.; Sorensen, E. J., An expedient synthesis of maraviroc (UK-427,857) via C–H functionalization. *Tetrahedron Lett.* **2015,** *56* (23), 3620-3623.

23. Panel on Antiretroviral Guidelines for Adults and Adolescents. Guidelines for the use of antiretroviral agents in HIV-1-infected adults and adolescents. Department of Health and Human Services. Available at http://aidsinfo.nih.gov/contentfiles/lvguidelines/AdultandAdolescentGL.pdf. Section accessed 3/15/17.

24. Cox, B. D.; Prosser, A. R.; Sun, Y.; Li, Z.; Lee, S.; Huang, M. B.; Bond, V. C.; Snyder, J. P.; Krystal, M.; Wilson, L. J.; Liotta, D. C., Pyrazolo-Piperidines Exhibit Dual Inhibition of CCR5/CXCR4 HIV Entry and Reverse Transcriptase. *ACS Med. Chem. Lett.* **2015,** *6* (7), 753-757.

25. Brechtl, J. R.; Breitbart, W.; Galietta, M.; Krivo, S.; Rosenfeld, B., The use of highly active antiretroviral therapy (HAART) in patients with advanced HIV infection: impact on medical, palliative care, and quality of life outcomes. *J. Pain Symptom Manage.* **2001,** *21* (1), 41-51.

26. Cavrois, M.; de Noronha, C.; Greene, W. C., A sensitive and specific enzyme-based assay detecting HIV-1 virion fusion in primary T lymphocytes. *Nat. Biotech.* **2002,** *20* (11), 1151-1154.

27. Flexner, C., HIV drug development: the next 25 years. *Nat. Rev. Drug Discov.* **2007,** *6* (12), 959-966.

28. L.A. Kohlstaedt, J. W., J.M. Friedman, P.A. Rice, T.A. Steitz, Crystal Structure at 3.5 A Resolution of HIV-1 Reverse Transcriptase Complexed with an Inhibitor. *Science* **1992,** *256*, 1783-1790.

29. Liu, T.; Li, X.; You, S.; Bhuyan, S. S.; Dong, L., Effectiveness of AMD3100 in treatment of leukemia and solid tumors: from original discovery to use in current clinical practice. *Exp Hematol Oncol.* **2016,** *5* (1), 19.

30. Washington, K.; Miller, R., *Health Care Business Market Research Handbook*. 19th ed.; Richard K. Miller and Associates: Norcross (GA), 2017; p 552.